Nemo-like kinase suppresses Notch signalling by interfering with formation of the Notch active transcriptional complex

Ishitani, Tohru
Division of Cell Regulation Systems, Department of Post-Genome Science Center, Medical Institute of Bioregulation, Kyushu University

Hirao, Tomoko
Unit on Nervous Development Systems, Nagoya

Suzuki, Maho
Group of Signal Transduction, Laboratory of Cell Regulation, Division of Biological Science, Graduate School of Science, Nagoya

Isoda, Miho
Unit on Nervous Development Systems, Nagoya

他

出版情報：Nature Cell Biology. 12 (3), pp.278-285, 2010-03-01. Nature Publishing Group
バージョン：

Nemo-like kinase suppresses Notch signalling by interfering with formation of the Notch active transcriptional complex

Tohru Ishitani[1, 2, 4, 6], Tomoko Hirao[1], Maho Suzuki[2], Miho Isoda[1], Shizuka Ishitani[4], Kenichi Harigaya[5], Motoo Kitagawa[5], Kunihiro Matsumoto[2], & Motoyuki Itoh[1, 3, 6]

[1] Unit on Nervous Development Systems, [2]Group of Signal Transduction, Laboratory of Cell Regulation, Division of Biological Science, Graduate School of Science, [3] Institute for Advanced Research, Nagoya University, Nagoya 464-8602, Japan, [4] Division of Cell Regulation Systems, Department of Post-Genome Science Center, Medical Institute of Bioregulation, Kyushu University, Fukuoka 812-8582, Japan. [5]Department of Molecular and Tumor Pathology, Chiba University Graduate School of Medicine, Chiba 260-8670, Japan

[6]Correspondence should be addressed to T.I. or M.I. (e-mail: tish@bioreg.kyushu-u.ac.jp; mito@iar.nagoya-u.ac.jp)

The Notch signalling pathway plays a crucial role in determining cell fates in multiple tissues within metazoan organisms[1]. Upon binding to ligands, the Notch receptor is proteolytically cleaved and releases its intracellular domain (NotchICD). The NotchICD enters the nucleus and acts cooperatively with other factors to stimulate transcription of target genes. High levels of Notch-mediated transcriptional activation require the formation of a ternary complex consisting of NotchICD, CSL (CBF-1, suppressor of hairless, LAG-1), and a Mastermind family member[2-5]. However, how ternary complex formation is regulated remains largely unclear. Here we show that Nemo-like kinase (NLK) negatively regulates Notch-dependent transcriptional activation by reducing formation of this ternary complex. Using a biochemical screen, we identified Notch as a new substrate of NLK. NLK-phosphorylated Notch1ICD is impaired in its ability to form a transcriptionally active ternary complex. Furthermore, knockdown of NLK leads to hyperactivation of Notch signalling and consequently decreases neurogenesis in zebrafish. Our results both define a new function for NLK and reveal a novel mode of regulation in the Notch signalling pathway.

NLK is an evolutionarily conserved protein kinase that functions in various developmental events, such as *Drosophila* ommatidia rotation, *C. elegans* endoderm-induction, zebrafish brain AP-patterning, and mouse hematopoietosis[6-9]. NLK phosphorylates several transcription factors, including Lef1, c-Myb and STAT3[10-14]. In *Drosophila*, a mutant allele of *nemo* (the *Drosophila* NLK homologue) was identified in a screen for modifiers of activated Notch. In addition, another recent screen for Notch signalling modifiers also identified *nemo*[15, 16]. These studies suggest that *nemo* may participate in Notch signalling, but exactly how is not clear.

To further understand the molecular function of NLK, we searched for new NLK substrates using a biochemical screen (Fig. 1a, b, and see method section) and then identified Notch 3 as a novel NLK substrate (Fig. 1b). Four Notch members (Notch1-4) have been identified among vertebrates. These show considerable structural homology within their intracellular regions and share common domain architectures, including the RAM (RBP-Jκ-associated molecule) domain, the seven ankyrin repeats (ANK) domain, and a C-terminal PEST sequence[2]. Therefore, we hypothesized that NLK might phosphorylate and possibly regulate the activity of other Notch proteins in addition to Notch3. First, we examined whether NLK affects the transcriptional activity of each of the four mouse NotchICDs (Fig. 1c) by measuring activation of a Notch-responsive promoter (8x-wtCSL) containing multiple CSL binding sites following transient transfection of either wild-type or kinase-negative mutant of NLK into mouse neuroblastoma neuro-2a cells[17]. Activity of the 8x-wtCSL reporter was normalized against that of a reporter containing mutated CSL binding sites (8x-mtCSL). We found that Notch1ICD activity was repressed approximately 50% and 70% in cells transfected with 2.5 ng and 5 ng of an NLK expression plasmid, respectively, and that this activity required NLK kinase activity. In contrast, Notch2 and Notch4 activities were not significantly affected under the same conditions, while Notch3ICD activity was increased approximately 4 fold by wild-type but not by kinase-negative NLK. Since

NLK has a different effect on each of these four Notch activities in neuro-2a cells, we further examined if NLK affects the activities of Notch1ICD and Notch3ICD in other cell lines. We found that NLK repressed Notch1ICD activity 2- to 5-fold in four different cell lines examined (neuro-2a, SW480, HeLa, and HEK293), but regulated Notch3ICD activity in a cell line-dependent manner (Fig. S1). These data suggest that repression of Notch1ICD is a more generally conserved function of NLK in mammalian cells than modulation of Notch3ICD. This negative effect of NLK on Notch reporter activity is specifically mediated via Notch1ICD, because activation of the same reporter by CSL-VP16, which is constitutively active, was not affected by NLK (Fig. S2a). NLK also did not affect TNF-induced NF-κB reporter activity, suggesting that NLK does not repress the general transcriptional machinery (Fig. S2b).

We identified Notch3 but not Notch1 as an NLK substrate in our HEK293 screen. However, we observed that Notch3 is expressed at much higher levels than Notch1 in these cells (Fig. S3). We therefore tested if NLK binds to endogenous Notch1 using SW480 cells, which express detectable levels of both NLK and Notch1 (Fig. S3, S4). In this cell line, overexpressed NLK co-immunoprecipitated with endogenous full- and transmembrane- Notch1 (Notch1 TM) (Fig. S4a). Furthermore, co-immunoprecipitation of endogenous NLK with endogenous Notch1 TM was observed (Fig. S4b). Thus, the data suggest a physiological role for NLK in the negative regulation of Notch1. We next examined if endogenous NLK is involved in the regulation of Notch1 activity in neuro-2a cells and found that Notch1ICD activity was enhanced in cells in which NLK expression had been knocked down (Fig. 1d, S5). To further explore the contribution of endogenous NLK in Notch signalling, we used a co-culture assay consisting of NIH3T3 cells ectopically expressing Jagged1 or Jagged2 and SW480 cells, which express Notch1 but not Notch3 (Fig. S3). In these co-cultures, Notch reporter activity was stimulated 1.8- and 2.7- fold, respectively (Fig. 1e). Knockdown of NLK in SW480 cells enhanced these Jagged1- or Jagged2-induced Notch activities more than two-fold

(Fig. 1e, S6). This data showed that NLK plays a negative role in endogenous Notch1 signalling, and we focused our further investigations on the negative regulation of Notch1 by NLK.

We next observed that NLK interacted with and phosphorylated Notch1ICD in neuro-2a cells (Fig.2a, b). *In vitro* kinase assays further demonstrated that NLK can directly phosphorylate Notch1ICD (Fig. 2c). To determine which regions in Notch1ICD bind to and are phosphorylated by NLK, we examined *in vivo* phosphorylation (Fig. 2d, e) and NLK binding (Fig. S7) of a variety of *Xenopus* Notch1ICD fragments. We observed that NLK phosphorylated full-length ICD, ICD 22 (1751-2282) and ICD14 (2126-2524) but not ICD23 (1751-2125) or ICD15 (2282-2524) (Fig. 2e, bottom panel, lanes 4, 7, 10, 13, 16). NLK also bound to full-length ICD, ICD 22, and ICD23 but not to ICD14 (Fig. S7). These data suggest that NLK binds to the amino-terminal region (1751-2125) of Notch1ICD and phosphorylates the middle region (2126-2282) of Notch1ICD. Since NLK phosphorylates serine/threonine residues in the serine/threonine-proline motif (S/T-P)[11, 12], we searched for conserved S/T-P motifs around the middle region of vertebrate Notch1 proteins. We found seven such conserved S-P motifs (S1: S2118-P, S2: S2132-P, S3: S2137-P, S4; S2194-P, S5: S2211-P, S6: S2217-P, S7: S2222-P in *Xenopus* Notch1ICD) around this region (Fig. S8). To examine whether NLK phosphorylates these S-Ps, serine residues within these motifs were substituted to alanines (A). We observed that NLK still could bind to a mutant of *Xenopus* Notch1ICD, in which all 7 S-Ps had been changed to A-Ps (Notch1ICD-7A). However, NLK did not phosphorylate the Notch1ICD-7A mutant as efficiently as it did the wild-type Notch1ICD, suggesting that NLK phosphorylates the seven conserved S-Ps in the middle region of Notch1ICD (Fig. 2c).

Given that NLK antagonizes Notch1ICD activity, we next examined the effect of the Notch1ICD serine mutations on NLK-dependent transcriptional suppression.

Expression of NLK reduced the transcriptional activity of *Xenopus* Notch1ICD by 59 %, and this suppression was dependent on the kinase activity of NLK (Fig. 3a, b). Although NLK-mediated repression of *Xenopus* Notch1ICD was lower than that of mouse Notch1ICD (Fig.1c vs Fig. 3a, see also Fig. S9), these data show that the negative role of NLK in Notch1 regulation is conserved between these two species. NLK was significantly less effective in inhibiting transcriptional activity of Notch1ICD-7A (WT: 60% suppression; 7A:11% suppression, Fig. 3a, b), suggesting that Notch1ICD phosphorylation by NLK is required for reduction of Notch1 activity. We could not narrow down the particular residues involved in NLK-dependent inhibition of Notch1 activity because Notch1- 3A (S2118A, S2132A, S2137A) and -5A (S2118A, S2132A, S2137A, S2217A, S2222A) mutants were more sensitive to NLK than the 7A (all seven Ser residues to Ala) mutant (3A: 42% decrease; 5A: 24% decrease, Fig. 3a, b). These data suggest that phosphorylation of an exact sequence is not critical for NLK-mediated Notch inhibition. We next measured activity of Notch1ICD-7D, a mutant in which all seven serine residues had been changed to aspartic acid, which can mimic the charge of a phosphorylated serine. Notch1ICD-7D was less transcriptionally active than wild-type Notch1ICD (Fig. 3c). Furthermore, Notch1ICD-7D was less subject to inhibition by NLK than wild-type Notch1ICD (WT: 60% suppression; 7D: 37% suppression, Fig. 3c). Taken together, these data indicate that multiple S-Ps are involved in the suppression of Notch1 activity, and that phosphorylation of these serines in Notch1ICD plays a significant role in the negative regulation of Notch1 activity by NLK.

We next examined how NLK reduces Notch1ICD/CSL-mediated transcriptional activation. We observed that expression of NLK did not affect the stability of either transfected Notch1ICD or endogenous Notch1 (Fig. 2a, b, S5, S6, S10) or the nuclear localisation of Notch1ICD (Fig. S11). Activation of transcription by Notch signalling requires the recruitment of the transcriptional co-activator Mastermind into a ternary complex that contains Notch1ICD, CSL, and Mastermind[2]. We therefore examined

whether NLK interferes with formation of this complex in neuro-2a cells. Myc-tagged Notch1ICD was expressed with NLK or NLK-KN in neuro-2a cells and cell lysates were immunoprecipitated using anti-Myc antibody. This cell line expresses relatively high amounts of the CSL and Mastermind proteins, and thus the ternary complex can readily be detected by expression of Notch1ICD alone. The amount of co-precipitated endogenous CSL or Mastermind (MAML1, 2, and 3) was examined by immunoblot analysis. Wild-type NLK but not NLK-KN reduced the interaction between Notch1ICD and CSL or Mastermind (MAML1, 2, and 3) (Fig. 4a, S12, S13). In contrast, knockdown of NLK by siRNA in neuro2a cells increased Notch's ability to form complexes with CSL and MAML1 (Fig. 4b). Moreover, the Notch1ICD-7D mutant, which has weaker transcriptional activity, did not co-immunoprecipitate with MAML1 or CSL as efficiently as wild-type Notch1ICD in neuro2a cells (Fig. 4c). These data suggest the possibility that NLK-induced phosphorylation of Notch1ICD influences the ternary complex formation. To further investigate this possibility we used Notch1ICD, MAML1, and CSL proteins partially purified from HEK293 cells transfected with the corresponding expression plasmids, and combined these with control, wild-type NLK, or NLK-KN plasmids as indicated (Fig. 4d, e). By incubating different combinations of Notch1ICD, CSL, and MAML1 we observed that Notch1ICD and CSL spontaneously interact in the absence of NLK phosphorylation, whereas Notch1ICD and MAML1 interact only in the presence of CSL, suggesting the formation of a ternary complex containing MAML1 *in vitro* (Fig. S14, lanes 3, 7-9). In contrast, NLK-phosphorylated Notch1ICD protein formed a complex with CSL, but did not efficiently form a ternary complex with CSL and MAML1 (Fig. S14, lane 4). Interestingly, however, the interaction of Notch1ICD with CSL could also be inhibited by NLK *in vivo* (Fig. 4a). These results suggest that the Notch-CSL-Mastermind complex is much abundant than the Notch-CSL complex *in vivo*. Consistent with this, it has been shown that Mastermind stabilizes the DNA-binding complex consisting of Notch and CSL, thereby

forming a CSL-Notch- Mastermind complex in a cell line [4]. We further analysed formation of this complex by EMSA using DNA containing a *HES-1* promoter sequence[4]. Using the purified proteins mentioned above we found that CSL protein alone generated two bands, which presumably correspond to the CSL:DNA complex, and that addition of MAML1 did not affect this CSL:DNA complex (Fig. 4f, S15, white arrows). When we mixed Notch1ICD, MAML1, and CSL proteins, formation of the ternary complex was evident (Fig. 4f, lanes 3-5; S15, black arrows). However, NLK-phosphorylated Notch1ICD protein was less effective in forming the ternary complex on DNA (Fig. 4f, lanes 6-8). On the other hand, the Notch1ICD protein from cells co-transfected with NLK-KN was as effective as cells transfected with Notch1ICD alone in forming the ternary complex (Fig. 4f, lanes 3-5, 9-11). Furthermore, we performed EMSA using cell extracts from Notch1ICD and NLK-transfected neuro-2a cells. Cell extracts from mock-transfected cells generated a band that presumably corresponds to the CSL:DNA complex (Fig. S16c, white arrow). Upon transfection of Notch1ICD, formation of the ternary complex was evident (Fig. S16c, black arrow). This DNA/protein complex likely included CSL, Notch1, and Mastermind, since the band was supershifted by incubation with an anti-Notch1 antibody and the amount of the complex was increased, but the mobility was not altered after transfection of exogenous MAML1 (Fig. S16b, lane 2; Fig. S16c, black arrow). Transfection of NLK-WT but not NLK-KN with Notch1ICD reduced ternary complex formation on DNA (Fig. S16b, lanes, 2, 5, 8), suggesting that NLK reduces the formation of the ternary complex in an active kinase-dependent manner in neuro-2a cells. Taken together, these data suggest that NLK reduces the formation of the ternary complex by phosphorylating Notch1ICD.

In addition to Notch phosphorylation by NLK, we also found that NLK transfection produced a slower migrating band-shifted form of MAML1, suggesting phosphorylation of MAML by NLK (Fig. 4a, Fig. S16a). This raised the possibility that NLK may reduce ternary complex formation by phosphorylating MAML1. We therefore

investigated whether MAML1 also mediates the effect of NLK on complex formation. MAML1 was transfected with NLK and the cell lysates were mixed with lysates from Notch1ICD-transfected cells. We found that NLK did not affect the association of MAML1 with Notch1ICD (Fig. S17). Furthermore, purified NLK-phosphorylated MAML1 formed a ternary complex on DNA as efficiently as non-phosphorylated MAML (Fig. S18). Thus, the inhibitory effect of NLK on the complex formation is mediated by phosphorylation of Notch1ICD and not of MAML1.

To elucidate the *in vivo* role of NLK in regulating Notch, we used zebrafish as a model animal. We confirmed that zebrafish Nlk reduced zebrafish Notch1aICD- but not zebrafish Notch3- activity using the 8x-wtCSL reporter assay in neuro-2a cells, suggesting that the role of NLK in regulating Notch1 activity is conserved in zebrafish (Fig. S19). In early somite-stage zebrafish embryos, two Notch homologues, Notch1a and Notch3, cooperatively function to activate expression of the HES family of transcriptional repressors, such as *her4* and *hes5*, to represses primary neurogenesis[19, 20]. At this stage, *nlk* is expressed in the neural plate where primary neurogenesis occurs (Fig. S20a, b). These data suggest the possibility that Nlk is involved in Notch-regulated primary neurogenesis. To examine this possibility, we injected *nlk* mRNA or morpholino antisense oligonucleotides (MO) against the *nlk* gene into zebrafish embryos to ectopically activate or knock down *nlk* gene function, respectively. We then observed expression of the Notch target genes *her4* and *hes5*, as well as a marker of neuronal differentiation, *elavl3*. Knockdown of *nlk* increased the expression of both *her4* and *hes5* and decreased *elavl3*-expression (Fig. 5a, Fig. S21a, Table S1). In contrast, ectopic expression of *nlk* decreased expression of *her4* and increased that of *elavl3*, and these effects were partially dependent on Nlk kinase activity (Fig. S22). This suggests that Nlk positively regulates primary neurogenesis by repressing Notch signalling. We next tested whether negative regulation of *her4/hes5* expression by Nlk is mediated by Notch1a/3 in zebrafish embryos. In embryos injected with *notch1a/3*

MOs, expression of *her4* and *hes5* was reduced and that of *elavl3* expression was increased (Fig. 5a, table S1, ref. 20). Thus, Notch1a and Notch3 are involved in suppression of primary neurogenesis by activation of *her4* and *hes5* expression. Expression of *her4*, *hes5*, and *elavl3* in embryos co-injected with *notch1a/3* MOs and *nlk* MO were similar to those injected with Notch1a/3 MOs alone (Fig. 5a, Table S1). These data suggest that Nlk inhibits *her4/hes5* expression through the repression of Notch during zebrafish neurogenesis.

We further examined the effects of the Notch1ICD serine mutants on expression of Notch-regulated genes in zebrafish embryos by injection of their mRNAs. The Notch1ICD-7A mutant, which is insensitive to NLK-mediated phosphorylation, was more potent in inducing *her4* than wild-type Notch1ICD. In contrast, the Notch1ICD-7D mutant, which mimics the phosphorylated state, was less potent in inducing *her4* expression than wild-type Notch1ICD (Fig. 5b, Fig. S21). Accordingly, the Notch1ICD-7A mutant was similar to or more potent than wild-type Notch1ICD in repressing *elavl3* expression, whereas the Notch1ICD7D mutant was less potent than wild-type Notch1ICD in repressing *elavl3* (Fig. 5b, Fig. S21). Taken together, our data indicate that Notch phosphorylation by NLK plays an important role in repressing Notch activity and promoting neurogenesis in zebrafish embryos.

Based on these findings, we propose a model in which NLK antagonizes Notch signalling during (Fig. 5c, d). Upon ligand stimulation, full-length Notch1 is cleaved and Notch1ICD translocates into the nucleus. NLK can phosphorylate full-length Notch1 and Notch1ICD but does not affect the translocation of Notch1ICD. In cells with low or absence of NLK, a stable transcriptionally active complex (CSL, Notch, and Mastermind) efficiently forms (Fig, 5c). In contrast, in cells with high NLK kinase activity, the rate of the active complex formation is reduced (Fig. 5d). In neural progenitor cells, Notch activation induces HES-related genes and suppresses

neurogenesis. Thus, Notch inhibition by NLK promotes neuronal differentiation. The regulation of Notch activity by NLK may allow fine-tuning of the timing of neuronal differentiation *in vivo*. Consistent with our findings, NLK knockout mice suffer from various neurological abnormalities and overexpression of NLK induces neural development in *Xenopus*[21].

The NLK-phosphorylated region contains several previously identified functional domains, such as a serine/threonine rich (STR) region, and transactivation domain (TAD) (Fig. S8)[22-25]. Notch1 activity is suppressed by GM-CSF through a region that includes the STR. Although it is not known which kinases repress Notch1 activity, GM-CSF-induced phosphorylation of the STR region may interfere with ternary complex formation in a manner similar to that described here for NLK phosphorylation. The possible involvement of NLK in GM-CSF-mediated Notch1 repression remains to be determined in future studies. The C-terminal half of the NLK-phosphorylated domain in Notch proteins overlaps with their transactivation domain, called the TAD (S5-S7, Fig. S8) [25]. The TAD mediates the interaction between Notch and two HAT proteins, PCAF and GCN5. PCAF enhances Notch-mediated transcription from chromatin in collaboration with p300, another HAT protein that is recruited to the Notch complex by Mastermind [26]. Therefore, TAD may be involved in stabilizing a transcriptionally active complex consisting of Notch, Mastermind, and HAT proteins. NLK-mediated phosphorylation may interfere with this complex formation by affecting the interaction between these co-activator complexes and Notch. As mentioned above, the region in Notch proteins phosphorylated by NLK spans the STR and TAD domains. Our data suggest that the phosphorylation of Notch1ICD reduces the rate of ternary complex formation due to a conformational change around these domains. In addition, it is also possible that the phosphorylation of Notch may lead to recruit unknown factors which interfere with the formation of the ternary complex. Further studies are needed to assess these possibilities.

NLK-mediated repression requires phosphorylation on multiple sites and inhibition is roughly proportional to the number of phosphorylated sites. The exact site that is phosphorylated does not seem to be critical, but rather the number of negative charges provided by the phosphate group is important. Phosphorylation can alter the electrostatic properties of the residues around the sites of phosphorylation, and we imagine that graded changes in the phosphorylation pattern induced by NLK could alter the electrostatic properties around the ANK domain, whose seventh ankyrin repeat is just N-terminal to the NLK-phosphorylated region. Since the ANK domain of Notch forms an electrostatic (salt bridge) interaction with Mastermind and CSL[27, 28], phosphorylation-induced gradient increases in the electrostatic properties around ANK may inhibit the interaction between Notch and Mastermind proportional with the extent of phosphorylation. Similarly it has been proposed that multisite phosphorylation of proteins produce graded, additive changes in protein functions. For example, multiple phosphorylation sites within Ets1, a transcription factor, act additively to gradually increase DNA binding affinity[29]. Increasing the number of phosphorylation sites in smoothened (SMO), a signal transducer of Hedgehog signalling, results in a graded increase in SMO activity[30]. Taken together, our findings raise the possibility that the density of NLK phosphorylation sites in Notch serves as a molecular rheostat to fine-tune Notch activity.

Methods

Plasmids and antibodies.

Details for plasmids, reagents, and plasmid construction are provided in Supplementary Methods.

Cell culture and transfection.

HEK293 and neuro-2a cells were grown in Dulbecco's modified Eagle's medium supplemented with 10% fetal bovine serum. HEK293 cells were transfected with the expression plasmids by calcium phosphate precipitation or Polyethylenimine MW 25000 (Polysciences, Warrington, PA). Neuro-2a cells were transfected with the expression plasmids using FuGENE6 (Roche, Switzerland).

Immunoprecipitation and immunoblotting. Proteins from cell extracts were immunoprecipitated with various antibodies and protein G-Sepharose (GE, England). For immunoblotting, immunoprecipitates or whole-cell extracts were resolved by SDS-PAGE and transferred to Hybond-P membranes (GE, England). The membranes were immunoblotted with various antibodies, and the bound antibodies were visualized with horseradish-peroxidase-conjugated antibodies against rabbit or mouse IgG using ChemiLumi-one L chemiluminescent kit (Nacalai Tesque, Kyoto, Japan).

Identification of NLK substrates. Flag-NLK or NLK-KN proteins were obtained from HEK293 cells transfected with the corresponding expression plasmids. Cell lysates from 1×10^{10} HEK293 cells were pre-mixed without or with either Flag-NLK or NLK-KN protein. The mixtures were immunoprecipitated with anti-Flag and then washed 4 times with PBS(-). Half of the immunoprecipitate aliquot was subjected to an *in vitro* kinase assay and then separated by SDS-PAGE. Phosphorylated proteins were visualized by autoradiography. In parallel, the other half of the aliquots was also separated by SDS-PAGE, and then stained with CBB. Substrate candidates were cut out from the gel, and subjected to mass spectrometry using MS Voyager. Candidate proteins were identified by comparison of MS data against a protein sequence database.

***In vitro* kinase assays using NotchICD as a substrate.** Flag-NLK and NLK-KN were expressed in 293 cells and immunoprecipitated with anti-Flag antibody and protein G-Sepharose beads. Immunoprecipitates were purified by washing 5 times with PBS containing a high concentration of salt (0.625 M NaCl), and proteins were released from protein G-Sepharose beads using Flag peptides (Sigma). Myc-tagged Notch1ICD and its fragments were immunoprecipitated with anti-Myc antibody. Aliquots of immunoprecipitated NLK were incubated either without or with aliquots of immunoprecipitated NotchICD in 10 μl of kinase buffer containing γ^{32}P-ATP at 25°C for 5 min. Samples were resolved by SDS-PAGE, and phosphorylated proteins were visualized by autoradiography.

Reporter gene assays. Neuro-2a cells (2.5 x 10^5/well) were seeded into six-well (35-mm-diameter) plates. After 24 h, cells were transfected with the 8xwt-CSL-Luc or 8xmt-CSL-Luc reporter gene plasmids along with expression vectors as indicated. The total DNA concentration (1 μg/ml) was kept constant by supplementation with empty vector DNAs. Firefly and *Renilla* luciferase activities were determined with the Promega Dual luciferase assay system (Madison, WI). The pRL-EF vector (1 ng), which expresses *Renilla* luciferase under the control of the EF-1α promoter, was used for normalizing transfection efficiency of the luciferase reporters. In NotchICD/CSL-dependent reporter assays, 8xwt-CSL activities were normalized against 8xmt-CSL activities. In co-culture reporter assays, SW480 (2 x 10^5) cells were transfected with control or two different NLK siRNAs (10 nM), and 24 hours later, cells were further transfected with TP1 plasmid (a Notch reporter plasmid, 0.5 μg) and pRL-EF (5 ng). Forty eight hours after siRNA transfection, SW480 cells were collected and split into three equal groups of 5 x 10^4 cells. These groups were then co-cultured with MIG- (control), Jagged1-, or Jagged2-expressing NIH3T3 (5 x 10^4) in 24 well plates for 48 hours, and luciferase activity was determined as described above. The values shown are

the averages of experiments repeated three times, with each transfection performed in duplicate per experiment.

Phosphatase treatment. Cell lysates were incubated with or without λ-protein phosphatase (Cell signaling, Beverly, MA) at 30°C for 30 min.

NLK siRNA. Mouse NLK siRNA oligonucleotides (sense: GAACCUCAGCUCUGUCCGAtt, antisense: UCGGACAGAGCUGAGGUUCtt) were obtained from Gene-net (Fukuoka, Japan). Negative control siRNA oligonucleotides for the mouse cell line were obtained from B-bridge (Mountain View, CA). Human NLK siRNA oligonucleotides #1, #2, and their negative control siRNA oligonucleotides were obtained from Integrated DNA Technologies (Coralville, IA). For RNAi in neuro-2a cells, siRNA oligomers (final 20 nM) were transfected 2 times into cells using Lipofectamine RNAi MAX (Invitrogen, Carlsbad, CA). For RNAi in SW480 cells, siRNA oligomers (final 10 nM) were transfected into cells using Lipofectamine RNAi MAX.

Preparation of purified proteins. Flag-tagged MAML1 and Flag-tagged CSL with full coding sequences for each of the protein were expressed in 293 cells and immunoprecipitated with anti-Flag antibody-conjugated agarose beads (Sigma). Myc-tagged mouse Notch1ICD was expressed without or with either Flag-NLK WT or KN in 293 cells and immunoprecipitated with anti-Myc antibody-conjugated agarose beads (MBL, Japan). Immunoprecipitates were purified by washing 5 times with PBS containing 0.625 M NaCl (high salt) instead of the standard concentration of 0.125 M NaCl and proteins were released from agarose beads using either Flag peptides (Sigma) or Myc peptide (MBL).

Electrophoretic mobility shift assays (EMSA). Purified proteins were prepared as above. For EMSA using purified proteins, the indicated amounts of each protein were incubated with the ^{32}P-labelled CSL binding sequences derived from the mouse *HES-1* promoter[4] in 20 μl of binding buffer (13 mM Hepes-NaOH pH 7.9, 50 mM NaCl, 2 mM

MgCl2, 8% Glycerol, 2.5mM DTT, 0.05% NP-40, 1.33 μg polydI:dC, 0.66 μg ssDNA, 4 μg BSA) for 30 minutes at 30°C. Half of the mixture was loaded on polyacrylamide gels (4%) in 0.5 x TBE buffer to separate DNA-protein complexes. Since CSL is the DNA-binding component of the Notch transcription complex, this assay can detect binding of the entire complex.

Zebrafish maintenance. Zebrafish were raised and maintained under standard conditions.

Morpholino and mRNA injections. Antisense morpholino oligonucleotides (MOs) were obtained from Gene Tools (Philomath, OR). The sequences of the *nlk* (zebrafish *nlk1*), *notch1a,* and *notch3* MOs were described previously[8, 20]. For all injections, 2-5 ng of *nlk* MO, 2-5 ng each of *nocth1a* MO and *notch3* MO, 100 pg of *Xenopus* Notch1ICD mRNA, or 200 pg of *nlk* mRNA were injected at the one-cell stage (in all Figures except Fig. 5b and S21) or two cell stage (in Fig. 5b and S22).

Whole-mount *in situ* hybridization. Digoxigenin-labelled RNA antisense probes were prepared from plasmids containing *nlk1*, *her4*, *hes5*, and *elavl3*.

Acknowledgement

We thank T. Honjo, T. C. Südhof, U. Lendahl, K. Yasutomo, C. Kintner, D. Hayward, J. D. Griffin, L. Wu, M. Takeichi, S. Chiba, A. Kikuchi, H. Fujisawa, and K. Hozumi for providing plasmid vectors, antibody, and cultured cells; H. Matsuo for technical assistance; H. Aiba laboratory members (especially, T. Sunohara) for technical advise; and J. Ninomiya-Tsuji for helpful discussions. This research was supported by Yamada Science Foundation (T.I.), Astellas Foundation for Research on Metabolic Disorders (T.I.), Program for Improvement of Research Environment for Young Researchers from SCF commissioned by MEXT of Japan (T.I. and M.I.), KAKENHI (19687013) from MEXT of Japan (T.I.), and the Grants-in-Aid for Scientific Research programs in Japan (K.M.and M.I.).

Reference

1. Artavanis-Tsakonas, S., Rand, M. D., & Lake, R. J. Notch signaling: cell fate control and signal integration in development. *Science* **284**, 770-776 (1999).

2. Bray, S. J. Notch signalling: a simple pathway becomes complex. *Nat. Rev. Mol. Cell Biol.* **7**, 678-689 (2006).

3. Wu, L., Aster, J. C., Blacklow, S. C., Lake, R., Artavanis-Tsakonas, S., & Griffin, J. D. MAML1, a human homologue of *Drosophila* mastermind, is a transcriptional co-activator for NOTCH receptors. *Nat. Genet.* **26**, 484-489 (2000).

4. Kitagawa, M., Oyama, T., Kawashima, T., Yedvobnick, B., Kumar, A., et al. A human protein with sequence similarity to *Drosophila* mastermind coordinates the nuclear form of notch and a CSL protein to build a transcriptional activator complex on target promoters. *Mol. Cell. Biol.* **21**, 4337-4346 (2001).

5. Oyama, T., Harigaya, K., Muradil, A., Hozumi, K., Habu, S., Oguro, H., Iwama, A., Matsuno, K., Sakamoto, R., Sato, M., Yoshida, N., & Kitagawa, M. Mastermind-1 is required for Notch signal-dependent steps in lymphocyte development in vivo. *Proc. Natl. Acad. Sci. U. S. A.* **104**, 9764-9769 (2007).

6. Choi, K. W., & Benzer, S. Rotation of photoreceptor clusters in the developing Drosophila eye requires the nemo gene. *Cell* **78**, 125-136 (1994).

7. Meneghini, M. D., Ishitani, T., Carter, J. C., Hisamoto, N., Ninomiya-Tsuji, J., *et al.* MAP kinase and Wnt pathways converge to downregulate an HMG-domain repressor in Caenorhabditis elegans. *Nature* **399**, 793-797 (1999).

8. Thorpe, C. J., & Moon, R. T. nemo-like kinase is an essential co-activator of Wnt signaling during early zebrafish development. *Development* **131**, 2899-2909 (2004).

9. Kortenjann, M., Nehls, M., Smith, A. J., Carsetti, R., Schuler, J., *et al.* Abnormal bone marrow stroma in mice deficient for nemo-like kinase, Nlk. *Eur. J. Immunol*. **31**, 3580-3587 (2001).

10. Ishitani, T., Ninomiya-Tsuji, J., Nagai, S., Nishita, M., Meneghini, M., *et al.* The TAK1-NLK-MAPK-related pathway antagonizes signalling between β-catenin and transcription factor TCF. *Nature* **399**, 798-802 (1999).

11. Ishitani, T., Ninomiya-Tsuji, J., & Matsumoto, K. Regulation of lymphoid enhancer factor 1/T-cell factor by mitogen-activated protein kinase-related Nemo-like kinase-dependent phosphorylation in Wnt/β-catenin signaling. *Mol. Cell Biol*. **23**, 1379-1389 (2003).

12. Kanei-Ishii, C., Ninomiya-Tsuji, J., Tanikawa, J., Nomura, T., Ishitani, T., *et al.* Wnt-1 signal induces phosphorylation and degradation of c-Myb protein via TAK1, HIPK2, and NLK. *Genes Dev.* **18**, 816-829 (2004).

13. Kojima, H., Sasaki, T., Ishitani, T., Iemura, S., Zhao, H., *et al.* STAT3 regulates Nemo-like kinase by mediating its interaction with IL-6-stimulated TGFβ-activated kinase 1 for STAT3 Ser-727 phosphorylation. *Proc. Natl. Acad. Sci. U. S. A.* **102**, 4524-4529 (2005).

14. Ohkawara, B., Shirakabe, K., Hyodo-Miura, J., Matsuo, R., Ueno, N., *et al.* Role of the TAK1-NLK-STAT3 pathway in TGF-β-mediated mesoderm induction. *Genes Dev.* 18, 381-386 (2004).

15. Verheyen, E. M., Purcell, K. J., Fortini, M. E., & Artavanis-Tsakonas, S. Analysis of dominant enhancers and suppressors of activated Notch in Drosophila. *Genetics* 144, 1127-1141 (1996).

16. Kankel, M.W., Hurlbut, G. D., Upadhyay, G., Yajnik, V., Yedvobnick, B., et al. Investigating the Genetic Circuitry of Mastermind in Drosophila, a Notch Signal Effector. *Genetics* 177, 2493-2505 (2007).

17. Zhou, S., Fujimuro, M., Hsieh, J. J., Chen. L., Miyamoto, A., *et al*. SKIP, a CBF1-associated protein, interacts with the ankyrin repeat domain of NotchIC to facilitate NotchIC function. *Mol. Cell Biol*. **20**, 2400-2410 (2000).

18. Kurooka, H., Kuroda, K., & Honjo, T. Roles of the ankyrin repeats and C-terminal region of the mouse notch1 intracellular region. *Nucleic Acids Res.* **26**, 5448-5455 (1998).

19. Takke, C., Dornseifer, P., v Weizsacker, E. & Campos-Ortega, J.A. *her4*, a zebrafish homologue of the *Drosophila* neurogenic gene E(spl), is a target of NOTCH signalling. *Development* **126**, 1811–1821 (1999).

20. Yeo, S., Kim, M. J., Kim, H., Huh, T., & Chitnis, A. B. Fluorescent protein expression driven by *her4* regulatory elements reveals the spatiotemporal pattern of Notch signaling in the nervous system of zebrafish embryos. *Dev. Biol.* **301**, 555-567 (2007).

21. Hyodo-Miura, J., Urushiyama, S., Nagai, S., Nishita, M., Ueno, N., et al. Involvement of NLK and Sox11 in neural induction in *Xenopus* development. *Genes Cells.* **7**, 487-496 (2002).

22. Gall, M. L. & Giniger, E. Identification of two binding regions for the suppressor of hairless protein within the intracellular domain of *Drosophila* Notch *J. Biol. Chem*. **279**, 29418-29426 (2004).

23. Bigas, A., Martin, D. I., & Milner, L. A. Notch1 and Notch2 inhibit myeloid differentiation in response to different cytokines. *Mol. Cell Biol.* **18**, 2324-2333 (1998).

24. Inglés-Esteve, J., Espinosa, L., Milner, L. A., Caelles, C., & Bigas, A. Phosphorylation of Ser2078 modulates the Notch2 function in 32D cell differentiation. *J. Biol. Chem.* **276**, 44873-44880 (2001).

25. Kurooka, H. & Honjo, T. Functional interaction between the mouse notch1 intracellular region and histone acetyltransferases PCAF and GCN5. *J. Biol. Chem*. **275**, 17211-17220 (2000).

26. Wallberg, A. E., Pedersen, K., Lendahl, U., & Roeder, R. G. p300 and PCAF act cooperatively to mediate transcriptional activation from chromatin templates by notch intracellular domains in vitro. *Mol. Cell Biol.* **22**, 7812-7819 (2002).

27. Wilson, J. J. & Kovall, R. A. Crystal Structure of the CSL-Notch-Mastermind Ternary Complex Bound to DNA. *Cell* **124**, 985-996 (2006).

28. Nam, Y., Sliz, P., Song, L., Aster, J. C., & Blacklow, S. C. Structural Basis for Cooperativity in Recruitment of MAML Coactivators to Notch Transcription Complexes. *Cell* **124**, 973-983 (2006).

29. Pufall, M. A., Lee, G. M., Nelson, M. L., Kang, H., Velyvis, A., Kay, L. E., McIntosh, L. P., & Graves, B. J. Variable Control of Ets-1 DNA Binding by Multiple Phosphates in an Unstructured Region. *Science* **309**, 142-145 (2005).

30. Zhao, Y., Tong, C., & Jiang, J. Hedgehog regulates smoothened activity by inducing a conformational switch. *Nature* **450**, 252-258 (2007).

Figure legends

Figure 1 Identification of Notch as a new NLK substrate.

(a) Flow chart of NLK substrate screening. (**b)** Identification of NLK substrates. Left panel shows the autoradiographic image from an *in vitro* kinase assay. Right panel shows the CBB-stained SDS-PAGE gel. Molecular weight marker sizes in kD are indicated between panels. The proteins that interact with NLK are indicated by open and closed arrows. NLK substrate candidates are indicated by closed and broken arrows. (**c**) NLK affects the activities of four Notch proteins differently. Expression plasmids (0.1 μg each of mouse Notch1ICD, Notch2ICD, Notch3ICD, Notch4ICD; 2.5 or 5 ng of NLK wild type (WT); 5 ng of NLK-KN (KN)) were transfected and the luciferase activities were measured in neuro-2a cells. Data from 8x-wtCSL reporters are normalized against those from 8x-mtCSL reporters. Activity of each NotchICD assayed in the absence of NLK was normalized to 100 %. (**d)** Knockdown of NLK increases Notch1 activity in neuro-2a cells. Neuro-2a cells were treated with either control siRNA or NLK siRNA before transfection of Myc-tagged Notch1ICD (Myc-Notch1ICD) (0.3 μg) and the Notch signalling reporter plasmids. The luciferase activity was measured as in **c**. Cell lysates were also immunoblotted with anti-Myc and anti-NLK antibodies (**d**). α-tubulin was used as a loading control. NLK siRNA reduces NLK protein levels. (**e**) NLK knockdown affect the endogenous protein levels of NLK but not Notch1 in SW480 cells. SW480 cells were treated with either control siRNA, NLK siRNA#1, or NLK siRNA#2. 24 hours later, cell lysates were immunoblotted with anti-Notch1 or anti-NLK antibody. α-tubulin was used as a loading control. The asterisk indicates a non-specific band, which was not reduced by NLK siRNA. (**f**) NLK knockdown increases Notch activity in SW480 cells. SW480 cells treated with siRNAs as indicated were transfected with the Notch signalling reporter plasmids (TP1). Twenty-four hours after transfection, the SW480 cells were split into three groups and each was co-cultured

with Jagged1- or Jagged2-expressing 3T3 cells (J1-3T3 or J2-3T3, respectively) or parental 3T3 cells (MIG3T3). After 48hours, cells were harvested and luciferase activity was measured.

Figure 2 NLK binds to and phosphorylates Notch1ICD.

(a) NLK binds to Notch1ICD. Neuro-2a cells were transfected with Flag-tagged NLK (Flag-NLK), Myc-tagged Notch1ICD (Myc-Notch1ICD) wild type (WT) and 7A mutant (7A) as indicated. Cell extracts were subjected to immunoprecipitation with anti-Flag antibody. Immunoprecipitated complexes were immunoblotted with anti-Myc and anti-Flag antibodies. NotchWT and 7A mutant bind equally to NLK. (**b**) NLK induces the phosphorylation of Notch1ICD *in vivo*. Neuro-2a cells were transfected with wild type NLK (WT), NLK-KN (KN), and Flag-tagged Notch1ICD (Flag-Notch1ICD) as indicated. Cell lysates were incubated with or without γ-protein phosphatase (PPase) and then immunoblotted with anti-Flag. Notch1ICD proteins migrated more slowly on SDS-PAGE when cells were transfected with NLK but not with NLK-KN. Treatment with phosphatase eliminated these slower migrating bands (pNotch1ICD). (**c)** NLK phosphorylates Notch1ICD *in vitro*. Myc-Notch1ICD WT, 7A mutant, and Flag-NLK were expressed in neuro2a cells and the proteins were purified. Aliquots of purified Notch1ICD and NLK were subjected to *in vitro* kinase assay. NLK phosphorylates Notch1ICD WT and, to a much lesser extent, the 7A mutant. Purified Notch1ICD and NLK proteins were confirmed by immunoblotting with anti-Myc or Flag antibody. **(d)** Schematic diagram of Notch1ICD constructs. (**e)** NLK phosphorylates the middle region of Notch1ICD. Myc-Notch1ICD, Flag-NLK wild type (WT), and Flag-NLK-KN (KN) were expressed and purified from HEK293 cells (upper left and right panels). Aliquots of purified Notch1ICD, Notch1ICD fragments, and NLK were subjected to *in vitro* kinase assay (lower panel). The arrow shows the band corresponding to autophosphorylated NLK.

Figure 3 NLK suppresses Notch signalling via Notch phosphorylation.
(a, **b, c)** Effect of serine mutations in Notch1ICD on NLK-mediated transcriptional inhibition. Neuro-2a cells were transfected with Notch signalling reporter plasmids and the expression plasmids encoding *Xenopus* Notch1ICD wild type (WT), Notch1ICD serine mutants (3A, 5A, 7A, and 7D) (0.5 μg), NLK wild type (WT) (0.1 μg) and NLK-KN (KN) (0.1 μg). After 24 hours, cells were harvested and luciferase activity was measured. In **a**, relative luciferase activity is shown. Data from 8x-wtCSL reporters are normalized against those from 8x-mtCSL reporters. Activities of each Notch1ICD-SA-mutant activity co-transfected with NLK-KN were normalized to 100 %. In **b**, the percentage suppression of the Notch1ICD constructs in Fig. 3a is shown. The percentage suppression was calculated by comparing the reporter activities from cells transfected with Notch1ICD and wild-type NLK versus the reporter activities from cells transfected with Notch1ICD and NLK-KN. In **c**, -fold activation is shown.

Figure 4 NLK reduces the Notch1ICD-CSL-Mastermind ternary complex formation.
(a) NLK reduces the interaction of Notch1ICD with CSL or MAML1. Neuro-2a cells were transfected with Myc-Notch1ICD, Flag-NLK wild type (WT), and Flag-NLK-KN (KN) expression plasmids. Cell extracts were immunoprecipitated with anti-Myc antibody. Immunoprecipitated complexes were immunoblotted with anti-CSL, anti-MAML1, and anti-Myc antibodies. Expression of CSL, MAML1, and Flag-NLK proteins in whole cell extracts was confirmed by immunoblotting with antibodies as indicated. (**b**) Knockdown of NLK increases the interaction of Notch1ICD with CSL or MAML1. Cell extracts from neuro-2a cells, which were transfected with NLK- or control- siRNA and Myc-Notch1ICD expression plasmid, were analyzed as in (a). (**c**) Seven serine-to-aspartic acid mutations in Notch1ICD reduce its interaction with CSL and MAML1. Cell extracts from neuro-2a cells, which were transfected with the

plasmids encoding Myc-Notch1ICD or Myc-Notch1ICD-7D, were analyzed as in (a). (**d-f)** NLK-mediated Notch1ICD phosphorylation reduces ternary complex formation on DNA. Myc-Notch1ICD proteins (A-C) were purified from HEK293 cells transfected with Notch1ICD without or with wild-type (WT) Flag-NLK or Flag-NLK-KN (KN) plasmids as indicated in **d**. Expression of Flag-NLK proteins in cell extracts was confirmed by immunoblotting with anti-Flag antibody in **d**. Arrowhead in **d** indicates the band corresponding to the purified Notch proteins. Flag-MAML1 and Flag-CSL proteins were purified from HEK293 cells transfected with Flag-MAL1 or Flag-CSL as indicated in **e**. The closed arrowhead, and the open arrowhead in **e** indicate purified CSL protein and purified MAML1 protein, respectively. Co-purified non-specific protein is indicated by the asterisk in **e**. In **f**, purified proteins were mixed as indicated and the complexes were examined for binding to the CSL elements of the HES-1 promoter by EMSA. The open arrowheads mark CSL-specific bands and the closed arrowhead marks the CSL-Notch1ICD-MAML1 complex-specific bands.

Figure 5 NLK promotes primary neurogenesis by inhibiting Notch signalling in zebrafish.

(**a**) Knockdown of Nlk leads to activation of HES gene expression and reduction of *elavl3* expression through Notch1a/3. Pictures show whole-mount *in situ* hybridization of 3-somite-stage zebrafish embryos uninjected or injected with *nlk*, *notch1a/3* MOs either alone or in combination as indicated, and stained for *her4*, *hes5*, or *elavl3*. Enlarged views of the yellow box areas are shown in the right panels. Panels show the dorsal views of the embryos, with the anterior to the left. Scale bar: 50 μm. (**b**) NLK-dependent phosphorylation of Notch1ICD affects Notch signalling and primary neurogenesis. Whole-mount *in situ* hybridization staining for *her4* or *elavl3* in 3-somite-stage zebrafish embryos injected with wild-type (WT) Notch1ICD, 7A, or 7D mRNA (*her4*: total number (n) of WT, 7A, 7D injected embryos = 108, 119, 100, respectively;

elavl3: n of WT, 7A, 7D = 108, 103, 103, respectively). The number is the total number of embryos from three independent experiments. Panels show the dorsal views of the embryos, with the anterior to the top. Each mRNA was injected into one of two blastomeres (the right side of the embryos). Embryos were classified into three groups based on the expression levels of *her4* (++: greatly induced, +: slightly induced, no effect) or *elavl3* (--: greatly decreased, -: slightly decreased, no effect). Percentages of embryos with relative expression levels are indicated in the upper left corner of each panel. (**c**, **d**) A model for the role of NLK in suppression of ternary complex formation through NotchICD phosphorylation. (c) Ligands binding stimulates the release of Notch1ICD from full-length Notch1. Notch1ICD translocates into the nucleus, where it forms the active ternary complex. The complex induces *her4* and suppresses neurogenesis during zebrafish development. (d) In cells with NLK, Notch1ICD can be phosphorylated by NLK either at the membrane before it is cleaved from the full-length Notch1, or in the nucleus. The phosphorylation of Notch1ICD reduces the rate of the complex formation by inducing a conformational change in Notch. NLK-mediated phosphorylation of Notch helps promote neurogenesis by reducing Notch activation.

Supplementary methods

Expression vectors and antibodies. 8xwt-CSL, 8xmt-CSL, and TP1-luciferase reporter [31], antisense probes for *nlk* (*nlk1*), *her4*, *hes5*, and *elavl3*, and expression plasmids carrying NLK, Mastermind, mouse NotchICDs (in Fig. 1c, 2b, 4d-f, S1, S2, S9, S11, S16, and S18), human Notch1ICD (in Fig. S16), *Xenopus* Notch1ICD (in Fig. 1d, 2a, 2c-e, 3, 4a-c, 4g, S5, S7, S9, S10, S14, and S17) and its fragments have been described previously[3, 10, 12, 17, 25, 32-38.] Notch1ICD mutants, 3A, 5A, 7A, and 7D were created by introducing the corresponding mutations into *Xenopus* Notch1ICD using site-directed mutagenesis. Anti-Myc (9E10 and A14), anti-HA (Y11), anti-Notch1 (mN1A, sc-6014-r, and sc-6014), anti-Notch3 (M-134), and anti-Notch4 (sc-5594) antibodies were obtained from Santa Cruz (Santa Cruz, CA). Anti-Flag (M2) antibody was obtained from Sigma (St. Louis, MO). Anti-MAML1/2/3 antibodies were obtained from Bethyl (Montgomery, TX).Anti-CSL antibody was obtained from the Institute of Immunology (Tokyo, Japan). Anti-β-catenin was obtained from BD Biosciences (San Jose, California). Anti-NLK antibody was described previously[12-14].

RNA isolation and qRT–PCR. Embryos were injected with 100pg of Notch1ICD WT, 7A, 7D mRNA or *nlk* MO. At 11.5 hpf (5-somite stage), 50 embryos were collected and total RNA was purified by using standard Trizol and isopropanol precipitation. cDNA synthesis was performed using the Transcriptor High Fidelity cDNA Synthesis Kit (Roche, , Switzerland). Transcript levels of *her4*, *elavl3*, and *β-actin2* were quantified by real-time PCR using Power SYBR Mix (Applied Biosystems, CA) on a 7300 Real-Time PCR detection system (Applied Biosystems, CA). Results are expressed as the ratio relative to the housekeeping gene *β-actin2*. Primer sequences are as follows. *her4*(up) 5' CACACAGCAATGGCTCCTACA 3', *her4*(low) 5' ATGGGCTTTCTCAGCTTGTTTG 3', *elavl3*(up) 5' ATCACCTCACGCATCCTGGTA 3', *elavl3*(low) 5'

CTCCTCTGCTTCGTTCCGTTT 3', *β-actin2*(up) 5'
CTGACTGACTACCTCATGAAGATCCT 3', *β-actin2*(low) 5'
CCTTGATGTCACGGACAATTTC 3'.

Quantification of the ternary complex formation. Neuro-2a cells were transfected with the plasmids encoding Myc-Notch1ICD, Flag-NLK wild type (WT), and Flag-NLK-KN (KN). Cell extracts were immunoprecipitated with anti-Myc antibody. Immunoprecipitated complexes were immunoblotted with anti-CSL, anti-MAML1, and anti-Myc antibodies. Complex formation was quantified using Quantity One (Bio-Rad). The values shown are the averages of experiments repeated three times.

Electrophoretic mobility shift assays (EMSA). EMSA using cell extracts was performed as described[4]. For supershift experiments, anti-Notch1 or anti-β-actin (800 ng/lane) antibodies were included in the binding reaction.

Cell staining. Twenty-four hours after transfection of expression plasmids encoding Flag-NLK (0.06 μ g) and Myc-tagged Notch1ICDs (0.34 μ g), cells were fixed in 4% PFA and then permeabilized with 0.1% Triton X-100 in PBS for 2 min. The cells were then washed with PBS and incubated with PBS containing 10% FBS (blocking buffer) for 1 hour. To visualize the expression of NLK and Notch1ICDs, anti-Flag and anti-Myc were used as primary antibodies, respectively, and an Alexa488- or Alexa594-conjugated antibody (Invitrogen) was used as the secondary antibody. To visualize nuclei, DAPI (Dojin, Japan) was used. Images were acquired using an OLYMPUS BX51 microscope. More than 1000 cells were observed in two repeated experiments.

Cycloheximide treatment. Neuro-2a cells ($3x10^5$ cells) were transfected with Myc-tagged *Xenopus* Notch1ICD (0.5 μg) in the presence or absence of Flag-NLK (0.1 μg). Twenty-four hours after transfection, cells were treated with 25 ng/ml cycloheximide (Wako, Japan) for 4 or 8 hours, and then cell lysates were immunoblotted with anti-Myc and anti-Flag

Reference for supplementary methods

31. Minoguchi, S., Taniguchi, Y., Kato, H., Okazaki, T., Strobl, L. J., Zimber-Strobl, U., Bornkamm, G. W., & Honjo T. RBP-L, a transcription factor related to RBP-Jkappa. *Mol. Cell. Biol.* **17**, 2679-2687 (1997).

32. Mizutani, T., Taniguchi, Y., Aoki, T., Hashimoto, N., & Honjo, T. Conservation of the biochemical mechanisms of signal transduction among mammalian Notch family members. *Proc. Natl. Acad. Sci. U. S. A.* **98**, 9026–9031 (2001).

33. Shimizu, K., Chiba, S., Saito, T., Kumano, K., Hamada, Y., and Hirai, H. Functional diversity among Notch1, Notch2, and Notch3 receptors. *Biochem. Biophys. Res. Commun.* **291**, 775–779 (2002).

34. Lin, S. E., Oyama, T., Nagase, T., Harigaya, K., & Kitagawa, M. Identification of new human mastermind proteins defines a family that consists of positive regulators for notch signaling. *J. Biol. Chem.* **277**, 50612–50620 (2002).

35. Wettstein, D. A., Turner, D. L., & Kintner, C. The *Xenopus* homolog of *Drosophila* Suppressor of Hairless mediates Notch signaling during primary neurogenesis. *Development* **124**, 693-702 (1997).

36. Apelqvist, A., Li, H., Sommer, L., Beatus, P., Anderson, D. J., *et al*. Notch signalling controls pancreatic cell differentiation. *Nature* **400**, 877-881 (1999).

37. Raya,A., Kawakami,Y., Rodriguez-Esteban,C., Buscher,D., Koth,C.M., *et al*. Notch activity induces Nodal expression and mediates the establishment of left-right asymmetry in vertebrate embryos. *Genes Dev*. **17**, 1213-1218 (2003).

38. Kim, C. H., Ueshima, E., Muraoka, O., Tanaka, H., Yeo, S. Y., Huh, T. L. & Miki, N. Zebrafish *elav/HuC* homologue as a very early neuronal marker. *Neurosci. Lett*. **216**, 109 –112 (1996).

Legends for supplementary figures.

Figure S1 Inhibitory effect of NLK is specific to Notch1.

(a) Inhibition of Notch1 activation is a general function of NLK. Neuro-2a, SW480, HeLa, or HEK293 cells were transfected with Notch signalling reporter plasmids (8xwt-CSL-Luc or 8xmt-CSL-Luc reporter). Expression plasmids (0.3 μg each of mouse Notch1ICD, mouse Notch3ICD; 60 ng of wild-type (WT) NLK; 100 ng of NLK-KN (KN)) were transfected as indicated. Twenty-four hours after transfection, cells were harvested and luciferase activity was measured. Data from 8x-wtCSL reporters are normalized against those from 8x-mtCSL reporters. Notch1 activity is suppressed in all four cell lines by NLK but the effect of NLK on Notch3 is cell-line dependent. The data shown represent the mean of four independent experiments performed in duplicate and the error bars indicate the standard deviation. (**b**) NLK reduces Notch1-dependent but not Notch1-independent activation of the Notch reporter. (**c**) NLK does not affect NF-κB reporter activity. (**b**, **c**) Neuro-2a cells were transfected with either Notch signalling reporters (**b**) or a NF-κB reporter plasmid (**c**). Expression plasmids (0.3 μg each of mouse Notch1ICD; 0.3 μg each of VP16-CSL; 60 ng of NLK in **b**; 50 or 200 ng of NLK wild type (WT) in **b**; 100 or 400 ng of NLK-KN (KN)) were transfected as indicated. In **b**, twenty-four hours after transfection, cells were harvested and luciferase activity was measured. Data from 8x-wtCSL reporters are normalized against those from 8x-mtCSL reporters. In **c**, twenty-four hours after transfection, cells were treated with 10 ng/ml TNFα. After 6 hours incubation, cells were harvested and luciferase activity was measured. The data shown represent the mean of three (**b**) or four (**c**) independent experiments performed in duplicate and the error bars indicate the standard deviation.

Figure S2 Both overexpressed and endogenous NLK binds to endogenous Notch1 protein.

(a) Relative protein expression levels of Notch1 and Notch3. HeLa, HEK293, SW480, and neuro-2a cells were lysed, and then either immunoblotted with anti-Notch1 (sc-6014r), anti-Notch1 (mN1A), or anti-Notch3. α-tubulin was used as a loading control. (**b**) Relative mRNA expression levels of Notch1 and Notch3. Expression of Notch1 and Notch3 in HeLa, HEK293, or SW480 was assessed by quantitative RT-PCR. Two different primer sets (RT1 and RT2) for each gene were used for the analysis. The data shown represent the mean of two independent experiments performed in duplicate and the error bars indicate the standard deviation. HEK293 expresses a relatively high level of Notch3 but not Notch1 compared to other cells. (**c**) Flag-NLK binds to endogenous Notch1 protein. SW480 cells were transfected with Flag-NLK and Flag-NLK-KN as indicated. Cell extracts were subjected to immunoprecipitation with anti-Flag antibody. Immunoprecipitated complexes were immunoblotted with anti-Flag and anti-Notch1 (sc-6014r) antibodies. Flag-NLK binds to both endogenous full-length Notch1 (Notch1) and Notch1TM (TM). (**d**) Endogenous NLK binds to endogenous Notch1 protein. SW480, which expresses relatively high levels of Notch1 and NLK proteins (Fig S2a and S2b), were lysed, and then immunoprecipitated (IP) with either control IgG or anti-NLK. Immunoprecipitates and whole cell extracts were immunoblotted with anti-Notch1 (sc-6014r), anti-Notch1 (mN1A), and anti-NLK as indicated. Note that endogenous NLK bound to endogenous Notch1TM (TM).

Figure S3. The amino-terminal region of Notch1ICD is necessary for association with NLK.

HEK293 cells were transfected with Flag-NLK-KN, *Xenopus* Myc-Notch1ICD, and its derivatives (see Fig. 2d) as indicated. Cell extracts were subjected to immunoprecipitation with anti-Flag antibody. Immunoprecipitated complexes were immunoblotted with anti-Myc and anti-Flag antibodies. NLK binds to full-length Notch1ICD, Notch1ICD22, and Notch1ICD23 but not to Notch1ICD14.

Figure S4 Amino acid sequence alignment of the NLK phosphorylation regions among Notch proteins.

The amino-acid sequences of the NLK-phosphorylation regions within *Xenopus* Notch1 (xNotch1), zebrafish Notch1a (zNotch1a), zebrafish Notch3 (zNotch3), human Notch1 (hNotch1), mouse Notch1-4 (mNotch1-4), and *Drosophila* Notch (dNotch) were aligned using the MegAlign program (DNASTAR). Conserved residues are boxed. Red coloured boxes indicate the conserved serine residues. Seven SP motifs are conserved in human, mouse, and *Xenopus* Notch1 except zebrafish Notch1a (six out of seven are conserved). STR region and TAD are indicated by blue and orange boxes, respectively.

Figure S5. Mouse Notch1ICD is more sensitive to NLK-mediated suppression than *Xenopus* Notch1ICD.

Neuro-2a cells were transfected with Notch signalling reporter plasmids (8xCSLwt/mt-Luc). Expression plasmids (0.3 μg each of mouse and *Xenopus* Notch1ICDs, 60 ng of NLK wild type (WT), and 100 ng of NLK-KN (KN)) were transfected as indicated. Twenty-four hours after transfection, cells were harvested and luciferase activities were measured. Data from 8x-wtCSL reporters were normalized against those from 8x-mtCSL reporters. The data shown represent the mean of three independent experiments performed in duplicate and the error bars indicate the standard deviation.

Fig. S6 NLK does not alter the protein stability of Notch1ICD. Neuro-2a cells were transfected with Myc-tagged *Xenopus* Notch1ICD and Flag-NLK as indicated. Twenty-four hours after transfection, cells were treated with 25 ng/ml cycloheximide (CHX) for the indicated time periods, and then cell lysates were immunoblotted with anti-Myc and anti-Flag. α-tubulin was used as a loading control. β-catenin protein level was

decreased in the presence of CHX, confirming inhibition of protein synthesis. Amounts of Notch1ICD and α-tubulin proteins were quantified using Quantity One (Bio-Rad). Relative Notch1ICD protein levels were calculated by determining the ratio of Notch1ICD to α-tubulin at indicated time points and are presented as percentages of the Notch1ICD protein levels in untreated cells below panels.

Fig. S7 NLK does not alter the subcellular localization of Notch1ICD.
Neuro-2a cells were transfected with Myc-tagged *Xenopus* Notch1ICD wild-type and 7D mutant, mouse Notch1ICD, and Flag-NLK as indicated. Twenty-four hours after transfection, the localization of Notch1ICD and NLK were examined by staining with anti-Myc (red) and anti-Flag (green) antibodies, respectively. Nuclei were visualized with DAPI (blue). Cells were classified into two group based on the Notch1ICD localization [black: nucleus (++) / cytoplasm (-), red: nucleus (+) / cytoplasm (+)]. Scale bar (white line): 10 μ m.

Figure S8 NLK affects the formation of Notch1ICD ternary complex.
(a, **b**) Neuro-2a cells were transfected with Myc-Notch1ICD, wild-type Flag-NLK (WT) , and Flag-NLK-KN (KN) as indicated. Cell extracts were immunoprecipitated with anti-Myc antibody and then immunoblotted with anti-MAML2 in **a**, anti-MAML3 in **b**, and anti-Myc in **a** and **b**. Expression of MAML2, MAML3, and Flag-NLK proteins was confirmed by immunoblotting with anti-MAML2, anti-MAML3, and anti-Flag antibodies. (**c**) Quantification of Notch1ICD the binding to CSL, MAML1, MAML2, and MAML3. Neuro-2a cells were transfected with Myc-Notch1ICD, NLK wild type (WT), and NLK-KN (KN). Cell extracts were immunoprecipitated with anti-Myc antibody and then immunoblotted with anti-CSL, anti-MAML1, anti-MAML2, or anti-MAML3 and the amounts co-immunoprecipitated proteins quantified. Relative binding of Notch1ICD with each protein is shown. The values shown are the averages

of experiments repeated three times. (**d**) NLK interferes with CSL-Notch1ICD-MAML ternary complex formation, and this function depends on NLK kinase activity. Purified Flag-MAML1, Flag-CSL, and Myc-mouse Notch1ICD proteins were mixed and immunoprecipitated with anti-Myc antibody. The particular Myc-mouse Notch1ICD proteins examined were as follows: A, Myc-Notch1ICD purified from HEK293 expressing Myc-Notch1ICD alone; B, Myc-Notch1ICD purified from HEK293 expressing Myc-Notch1ICD and Flag-NLK; C, Myc-Notch1ICD purified from HEK293 expressing Myc-Notch1ICD and Flag-NLK KN. Flag-MAML1, Flag-CSL, and the immunoprecipitated complexes were then immunoblotted with anti-Flag and anti-Myc antibodies. Notch1ICD, MAML1, and CSL formed a ternary complex *in vitro* (lanes 3 and 9). CSL directly binds to Notch1 in a MAML1-independent manner (lane 8). MAML1 interacts with Notch1-CSL complex but not with Notch1 alone (lanes 7 and 9). NLK-phosphorylated Notch1ICD protein interacts with CSL, but interacts more weakly with MAML1 than unphosphorylated Notch1 ICD protein (lane 4 vs lanes 3, 5). (**e**) Purified Notch1ICD, MAML1, and CSL proteins are able to form a ternary complex on the CSL elements of the HES-1 promoter. Purified Notch1ICD, MAML1, and CSL proteins were mixed as indicated. The mixtures were subjected to EMSA using the CSL elements of the HES-1 promoter. The open arrowheads mark CSL-specific bands and the closed arrowhead marks the CSL–Notch1ICD-MAML1-specific band. (**f**-**h**) EMSA with cell extracts show that ternary complex formation on the CSL elements is reduced by NLK. (**f**) Cell extracts used for EMSA. Cell extracts (A-D) were prepared from neuro-2a cells transfected with Notch1ICD, wild-type Flag-NLK (WT), and Flag-NLK-KN (KN) plasmids. Expression of Notch1ICD, CSL, MAML1, and Flag-NLK proteins in cell extracts were confirmed by immunoblotting with the respective antibodies. (**g**) Cell extracts (B-D) were examined for binding activities to the CSL elements of the HES-1 promoter by EMSA (extract B, lanes 1-3; extract C, lanes 4-6; extract D, lanes 7-9). The open arrowheads mark the CSL-specific bands and the closed arrowheads

mark the CSL–Notch1ICD-Mastermind-specific bands. The asterisks indicate the CSL–Notch1ICD-Mastermind complexes, which are supershifted by anti-Notch1 antibody (lanes 2, 5, and 8). Note that co-expression of NLK reduces the amount of supershifted ternary complex. Anti-β-actin antibody was used as a control. (**h**) Transfected Notch1ICD can form a ternary complex with endogenous CSL and MAMLs in neuro-2a cells. Cell extracts were prepared from neuro-2a cells transfected with Notch1ICD and MAML1 plasmids either alone or in combination as indicated. The cell extracts were examined by EMSA as in **g**. The open arrowheads mark CSL-specific bands and the closed arrowheads mark the CSL–Notch1ICD-MAML1-specific band. Note that transfection of MAML1 increased the intensity of the CSL–Notch1ICD-MAML1-specific band but the mobility was the same as in the samples not transfected with MAML1. The band marked by the closed arrowhead should contain all of the CSL–Notch1ICD-MAML1, CSL–Notch1ICD-MAML2, and CSL–Notch1ICD-MAML3 complexes because the mobilities of these bands are indistinguishable on this gel[32], and all three endogenous MAML proteins are co-immunoprecipitated with Notch1ICD from extracts of cells transfected with Notch1ICD alone (Fig. 4a, S8a). (**i**) Phosphorylation of MAML1 by NLK is not required for the inhibition of the MAML1-NotchICD interaction. Neuro-2a cells were transfected with Flag-MAML1 and Flag-NLK plasmids either alone or in combination as indicated. The cell extracts were mixed with cell extract from Myc-Notch1ICD-transfected cells and then immunoprecipitated with anti-Myc antibody. Immunoprecipitated complexes were immunoblotted with anti-Flag and anti-Myc antibodies. Expression of Flag-MAML1 and Flag-NLK proteins in the cell extracts was confirmed by immunoblotting with anti-Flag antibody. (**j, k**) Phosphorylation of MAML1 does not affect the Notch1ICD-CSL-Mastermind ternary complex formation on DNA. **(i**) Purified proteins used in EMSA. Flag-MAML1 proteins (A, B) were purified from HEK293 cells transfected with Flag-MAML1 and HA-NLK expression plasmids as indicated. Arrowheads indicate purified MAML1

proteins. Expression of HA-NLK proteins in cell extracts was confirmed by immunoblotting with anti-HA antibody. (**k)** EMSA using purified proteins. Purified MAML1 (A, B), Flag-CSL (see Fig 4e), and Myc-Notch1ICD (A in Fig 4d) proteins were mixed as indicated and subjected to EMSA using the CSL elements of the HES-1 promoter. The open arrowheads mark CSL-specific bands and the closed arrowhead marks the CSL–Notch1IC-MAML1-specific band.

Figure S9 Zebrafish Nlk can suppress zebrafish Notch1a- but not Notch3-induced transactivation.

(a) Neuro-2a cells were transfected with Notch signalling reporter plasmids, Myc-tagged zebrafish Notch1a ICD (Myc-Notch1a ICD) (0.3 μg), Myc-tagged zebrafish Notch3ICD (Myc-Notch3 ICD) (0.3 μg), HA-tagged zebrafish Nlk (HA-Nlk) wild type (WT) (0.4 μg for zNotch1a; 0.3 or 1 μg for zNotch3) and kinase-negative mutant (KN) (0.4 μg for zNotch1a; 0.3 or 1 μg for zNotch3) plasmids as indicated. After 48 hours, cells were harvested and luciferase activities were measured. Data from 8x-wtCSL reporters were normalized against those from 8x-mtCSL reporters. The data shown represent the mean of four independent experiments performed in duplicate and the error bars indicate the standard deviation. (**b**) Expression of Myc-Notch1a-ICD, Myc-Notch3, and HA-Nlk was confirmed by immunoblotting with anti-Myc and anti-HA antibodies.

Figure S10 *nlk* and phosphorylation of Notch1ICD affect zebrafish primary neurogenesis.

(a) Expression of the *nlk* gene in 3-somite stage zebrafish embryos. Whole-mount *in situ* hybridization staining for *nlk*. Scale bar: 50 μm. (**b**) A transverse section of the neural plate showing *nlk* expression in 3-somite stage zebrafish embryos. The red broken line indicates the approximate border between the ectoderm and mesendoderm.

Scale bar: 50 μm. (**c**, **d**) Effects of Notch1ICD serine mutants or *nlk* MO on *her4*, *elavl3*, and *nlk* mRNA expression. Wild-type (WT), 7A, or 7D Notch1ICD mRNA or *nlk* MO was injected into one cell-stage zebrafish embryos. The relative expression levels of *her4*, *elavl3*, and *nlk* at the 5 somite stage was analyzed by quantitative RT-PCR in **c**. The values shown are the averages of three independent experiments and the error bars represent the SDs. (**d**) Expression of injected Notch1ICD proteins was monitored by immunoblotting with anti-Myc. (**e**, **f**) Effects of ectopic *nlk* expression on *her4* and *elavl3* expression in zebrafish embryos. Expression of *her4* is decreased, whereas *elavl3* is increased by expression of *nlk*, and these effects depend on Nlk kinase activity. Three somite-stage zebrafish embryos were either untreated or injected with *nlk* or with *nlk* kinase-negative (KN) mRNA and subjected to whole-mount *in situ* hybridization staining for *her4* or *elavl3* (*her4*: total number (n) of uninjected, *nlk*, *nlk-KN* injected embryos = 29, 69, 63, respectively; *elavl3*: n of uninjected, *nlk*, *nlk-KN* = 26, 65, 68, respectively). The number shown is the total number of embryos from two independent experiments. Panels show the dorsal views of the embryos, with the anterior to the top. Each mRNA was injected into one of two blastomeres (the right side of the embryos). Embryos were classified into two or three groups based on the expression of *her4* (no effect, decreased) or *elavl3* (decreased, increased, no effect). Percentages of embryos with relative expression levels are indicated in upper right corners of each panel. An enlarged view of an *nlk* mRNA-injected embryo is shown in **f**. Scale bar: 50 μm. Wild type *nlk* showed more potent *her4*-repressing activity and *elavl3*-inducing activity than *nlk-KN*, possibly through inhibition of Notch signalling. These data also indicate that NLK has some kinase activity-independent effects on these genes, because expression of either wild-type *nlk* or *nlk-KN* caused a reduction in both *her4* and *elavl3* expression in approximately 20% of the embryos. This kinase-independent function of Nlk remains uncharacterized.

Figure S11. Original western blots from figures 1, 2, and 4.

The original, uncropped western blot ilm scans are shown. Molecular weight markers are included. Figures 1d, 1e, 2a, 2b, 2c, 2e, 4a, 4b, 4c, 4d, and 4e are included.

Figure 1 Ishitani & Itoh

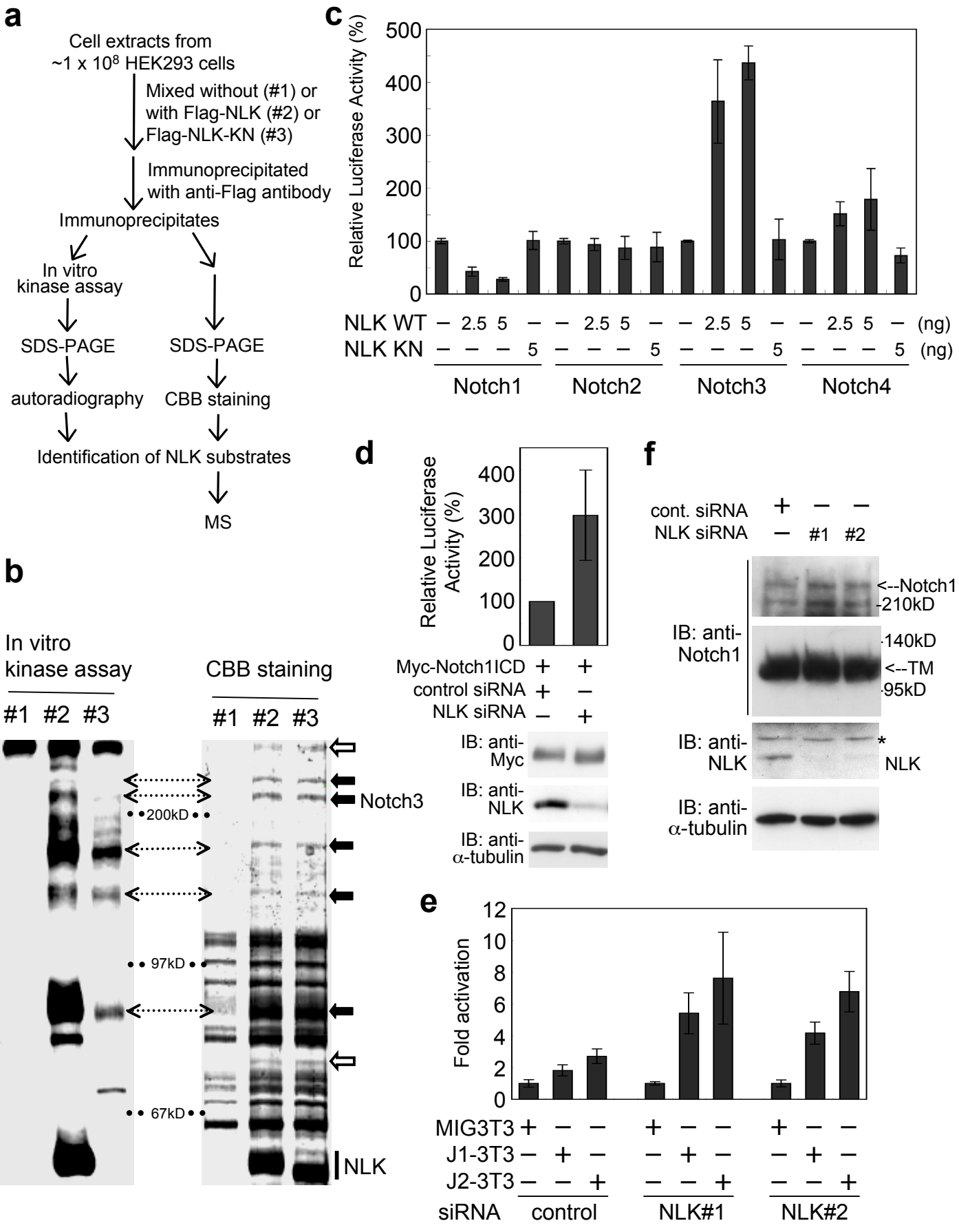

Figure 2 Ishitani & Itoh

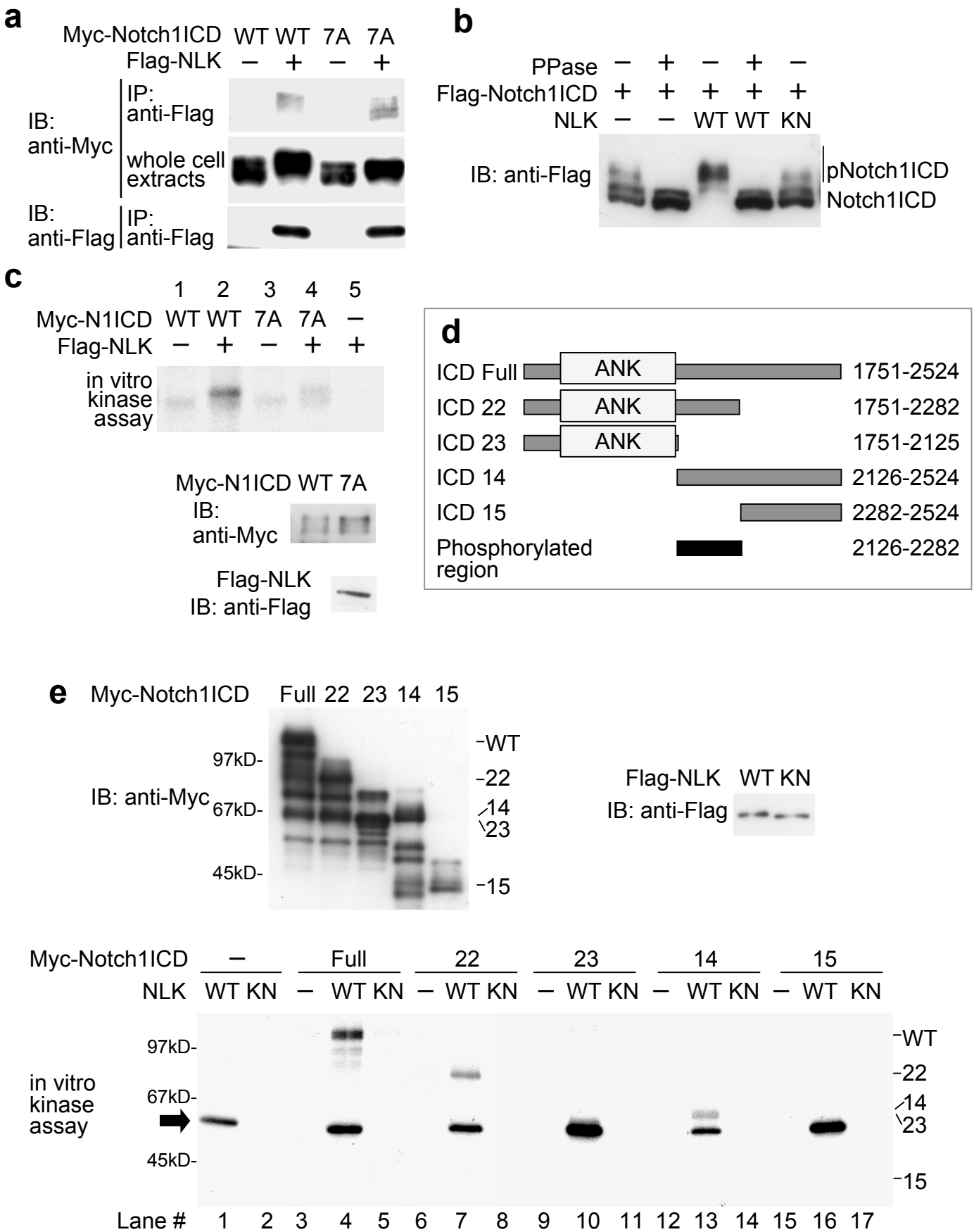

Figure 3 Ishitani & Itoh

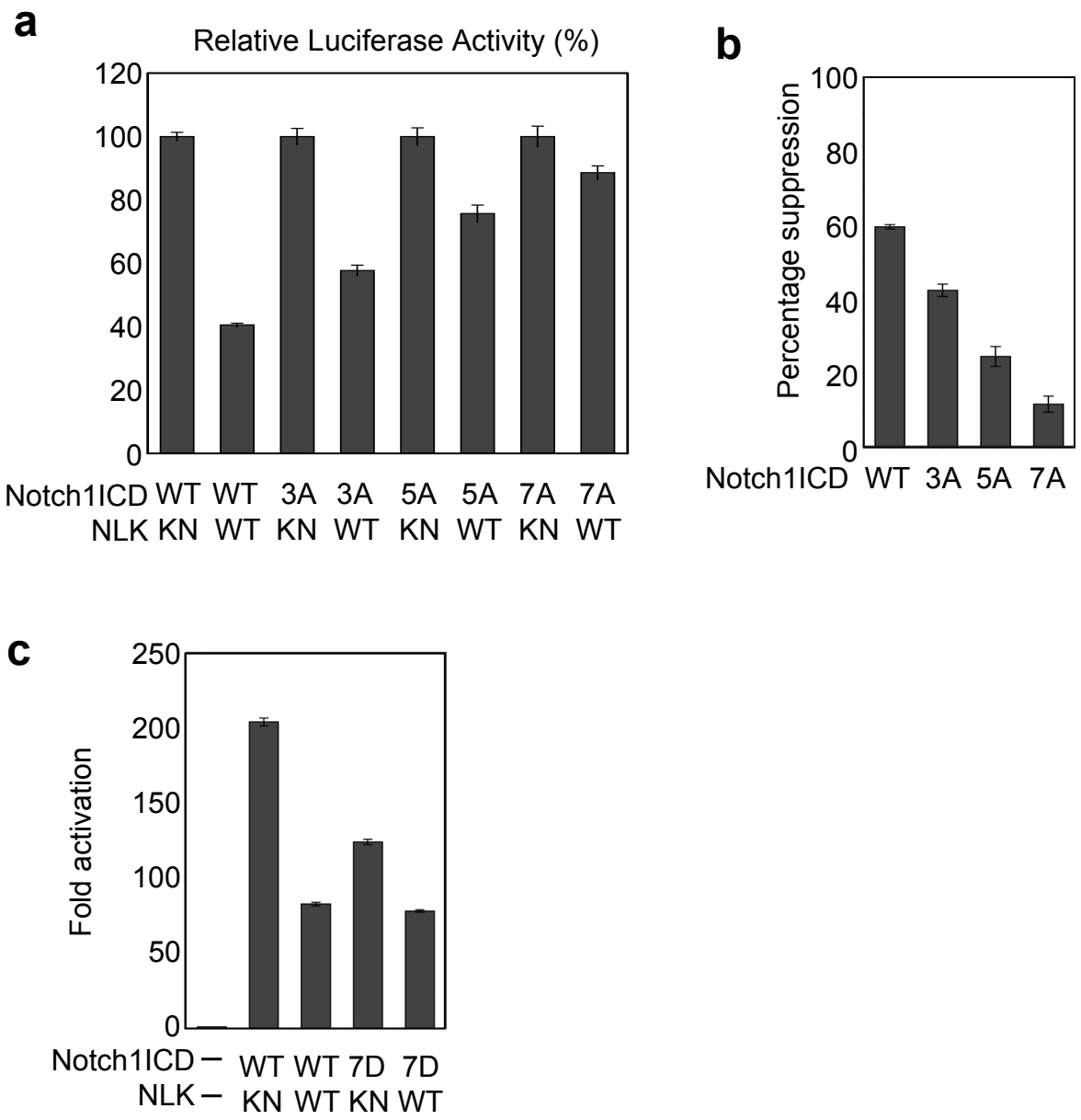

Figure 4 Ishitani & Itoh

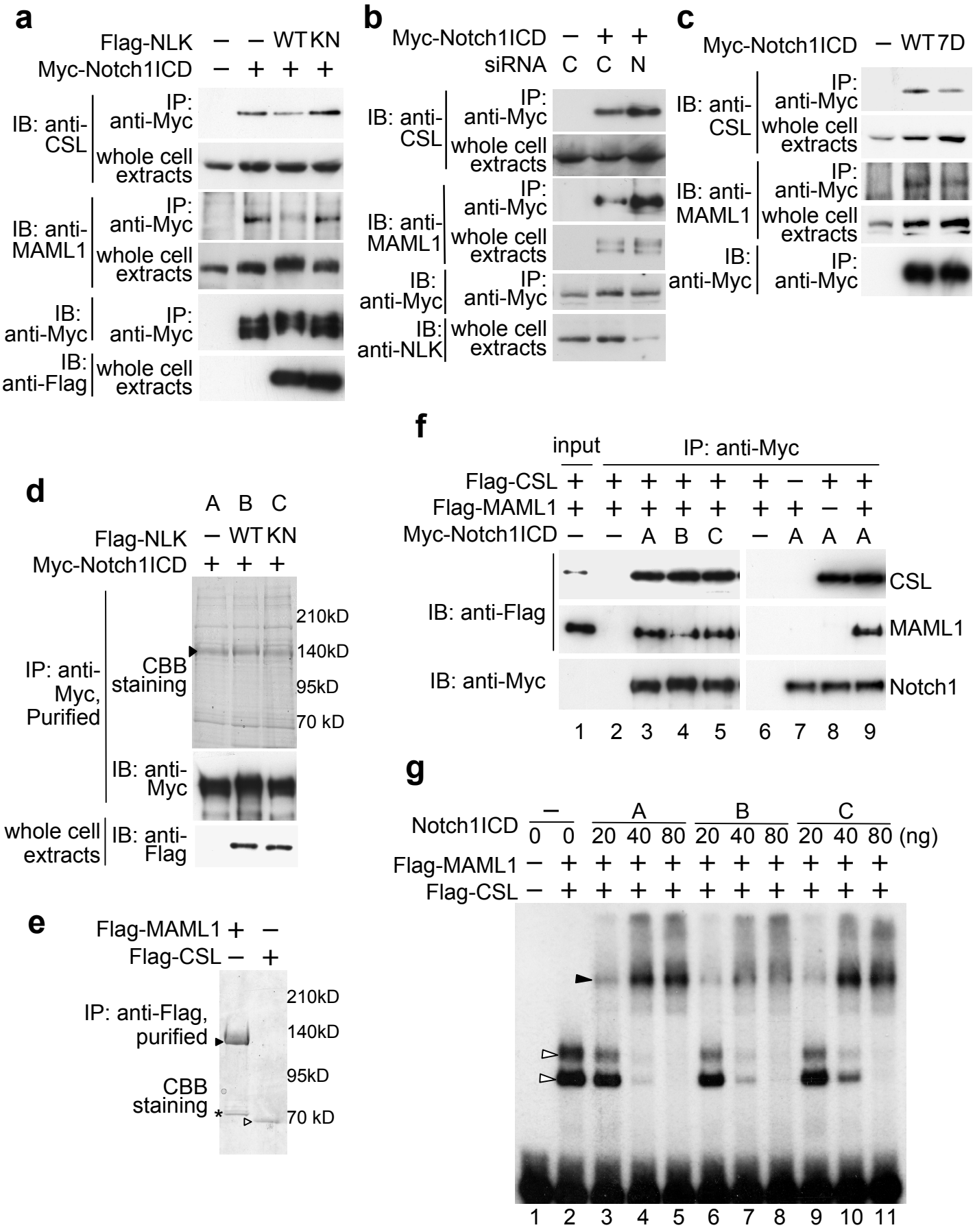

Figure S1 Ishitani & Itoh

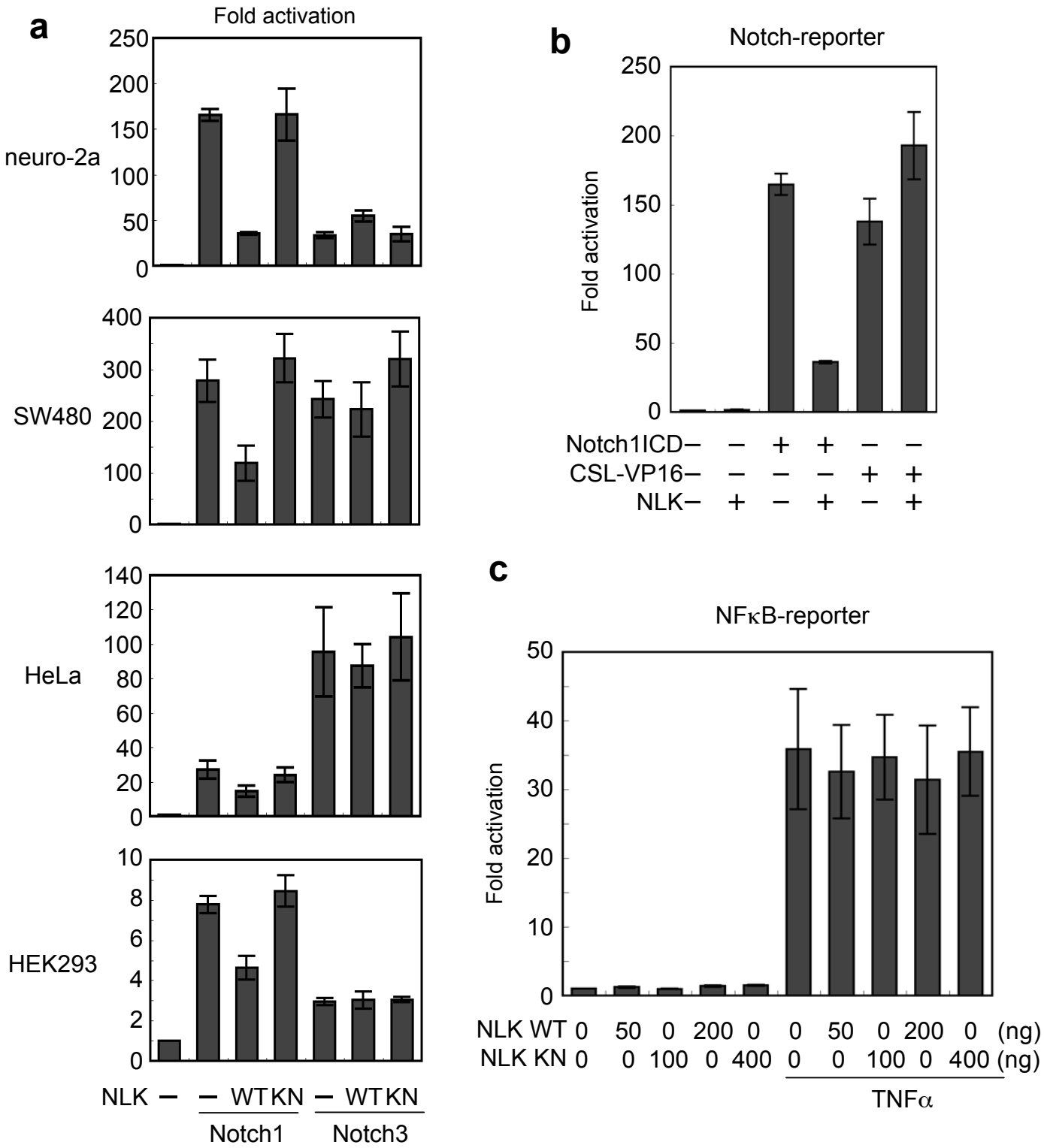

Figure S2 Ishitani & Itoh

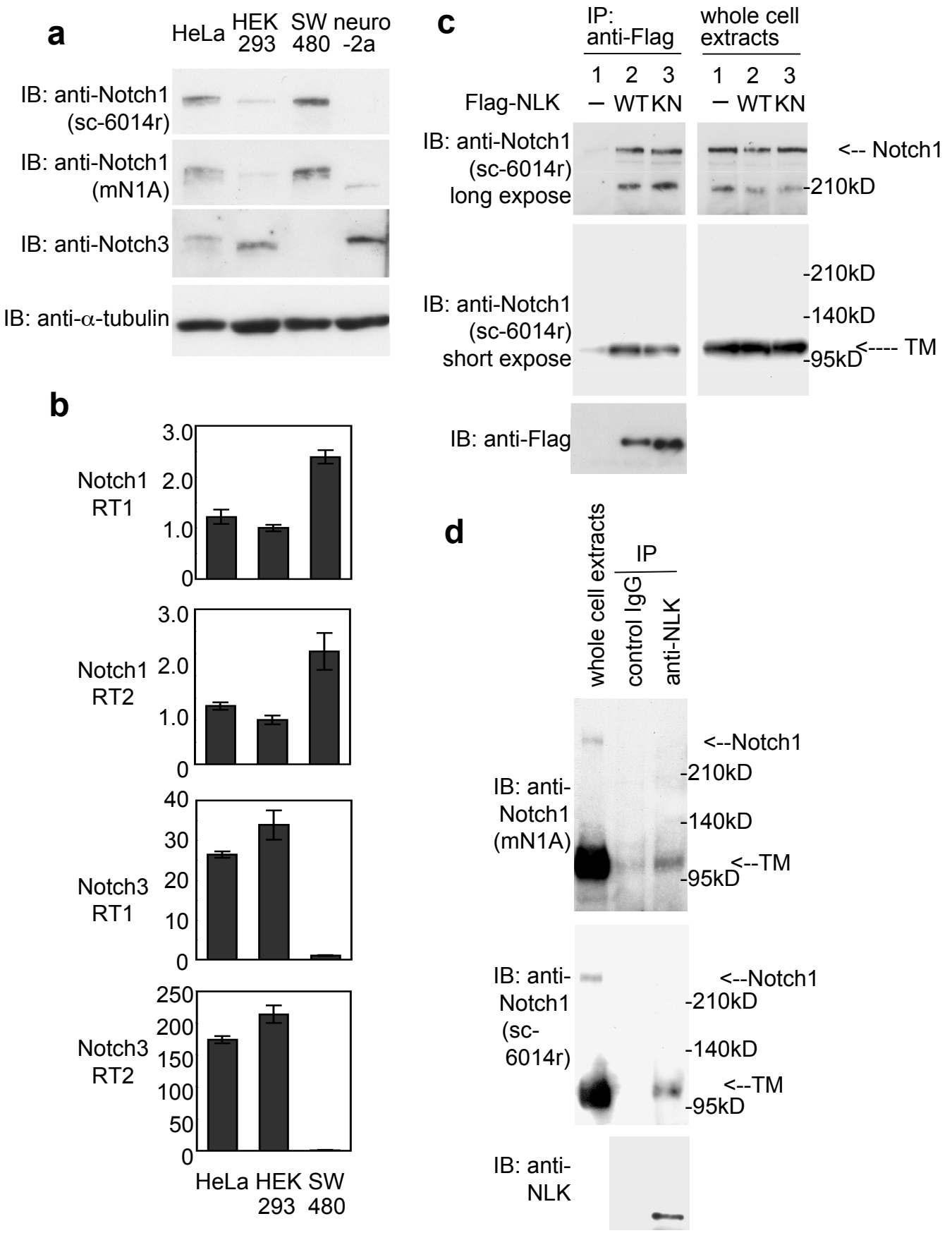

Figure S3 Ishitani & Itoh

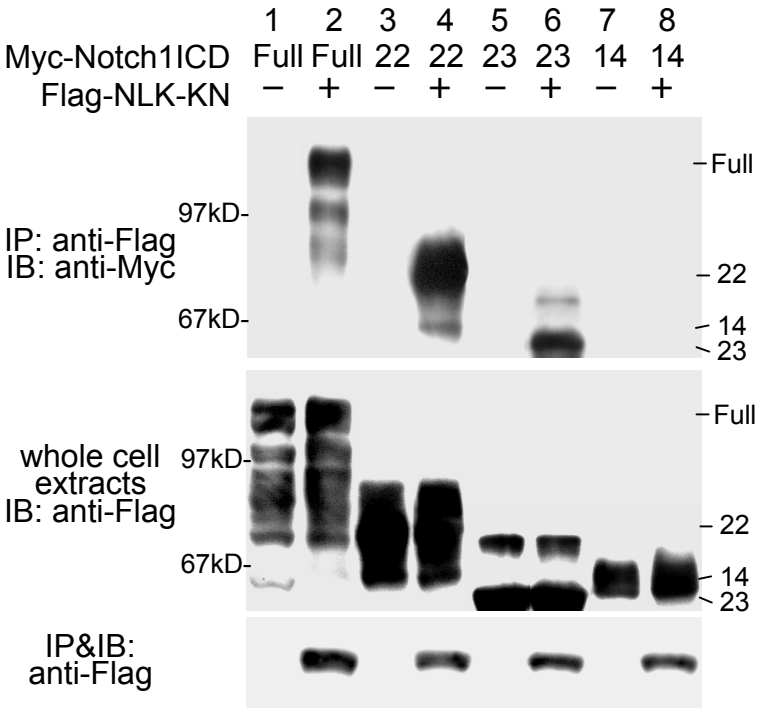

Figure S4 Ishitani & Itoh

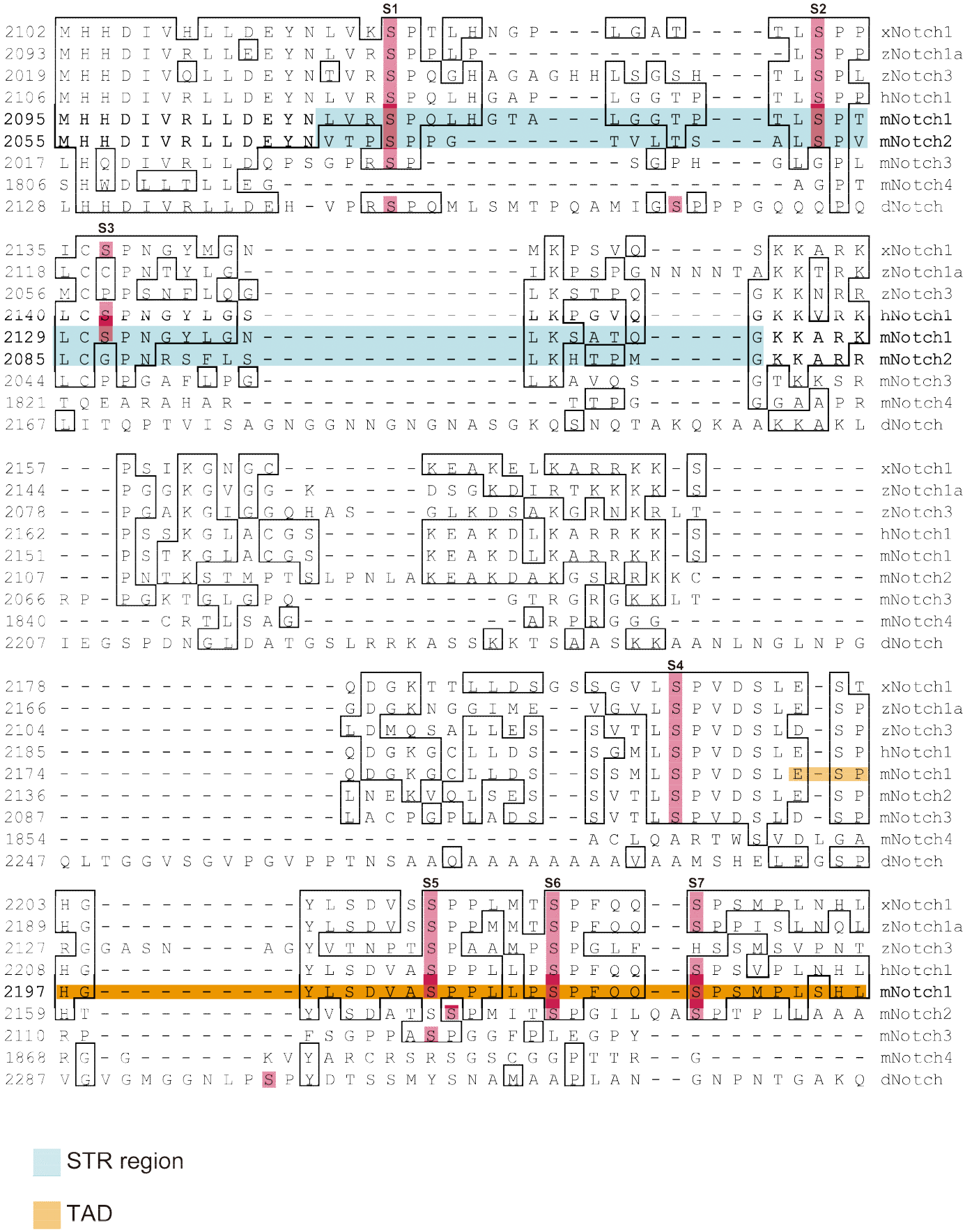

Figure S5 Ishitani & Itoh

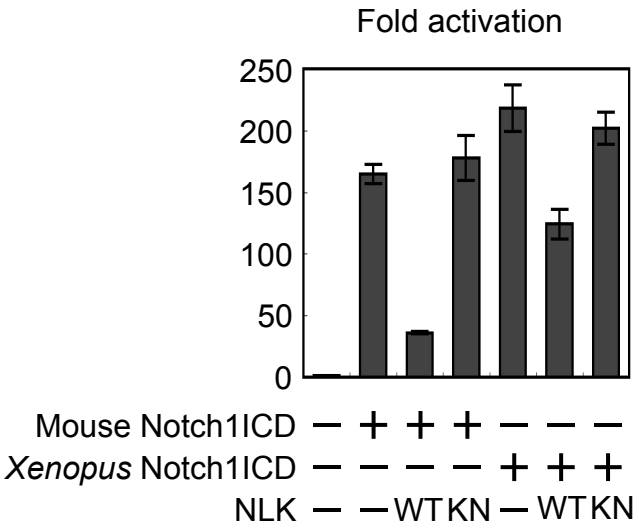

Figure S6 Ishitani & Itoh

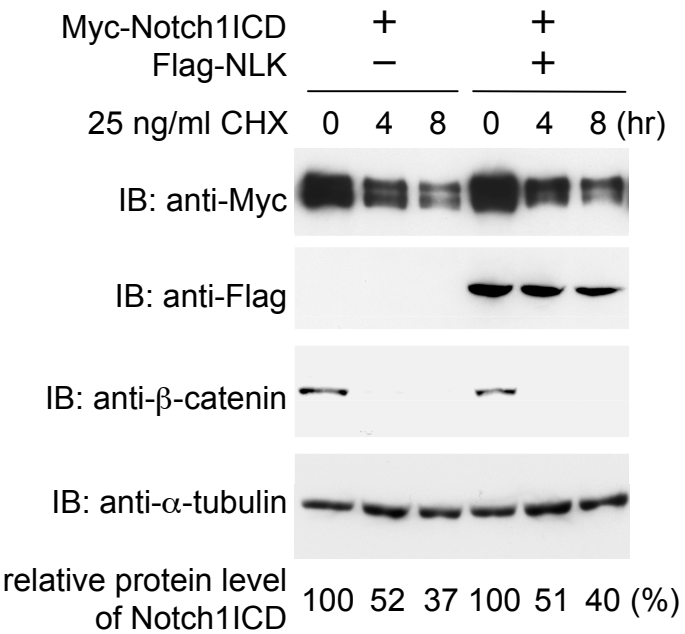

Figure S7 Ishitani & Itoh

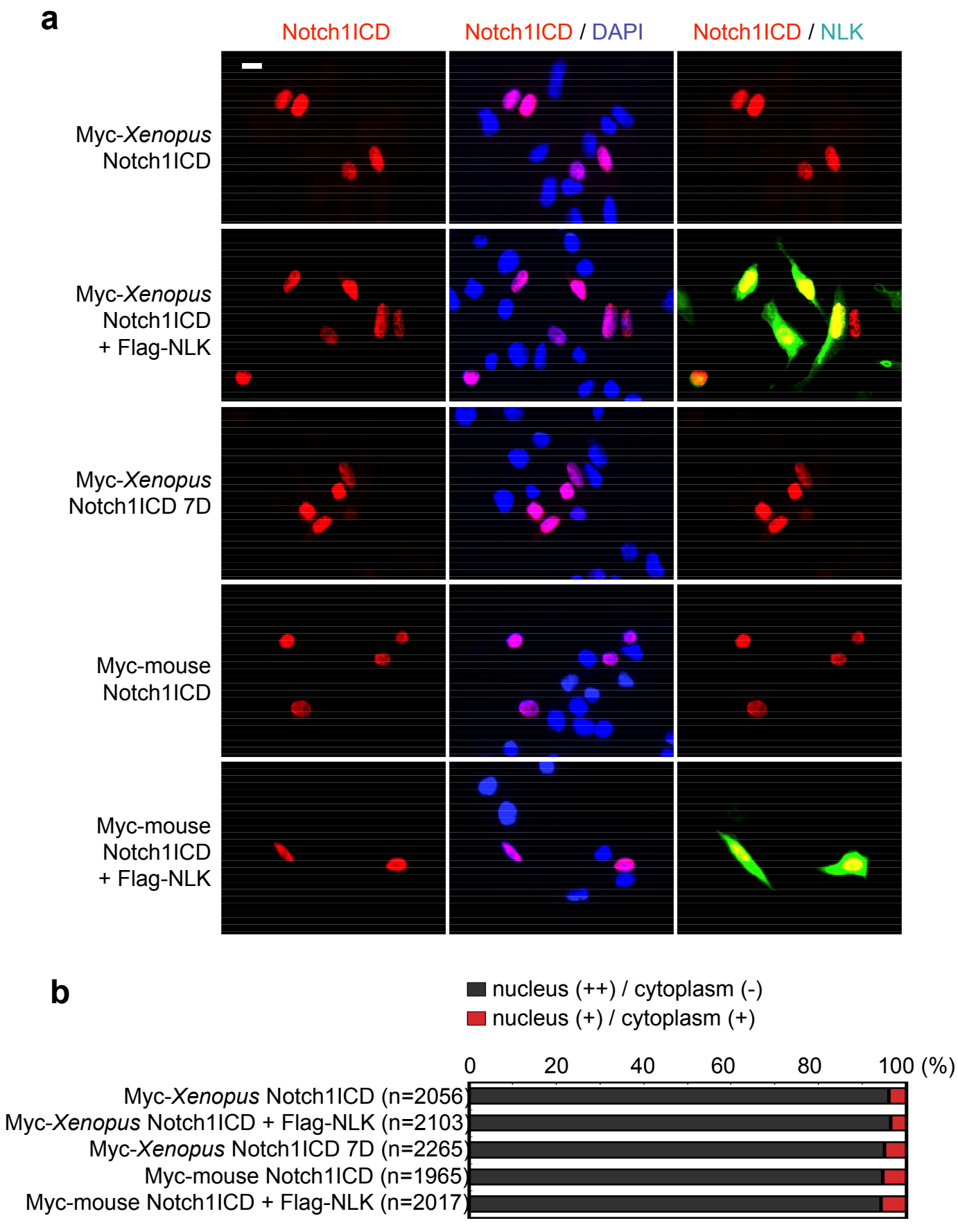

Figure S8 Ishitani & Itoh

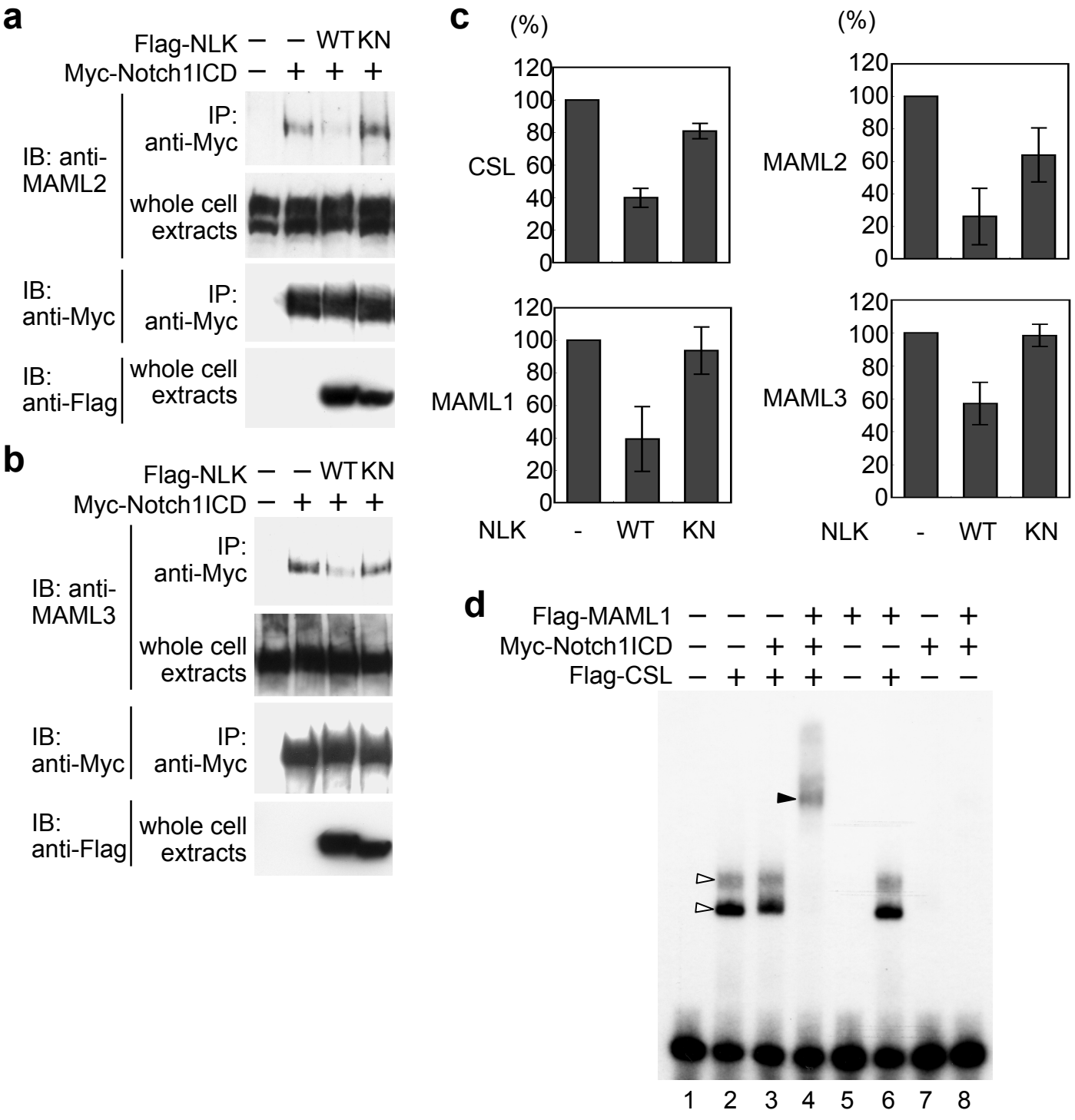

Figure S8 (continued)
Ishitani & Itoh

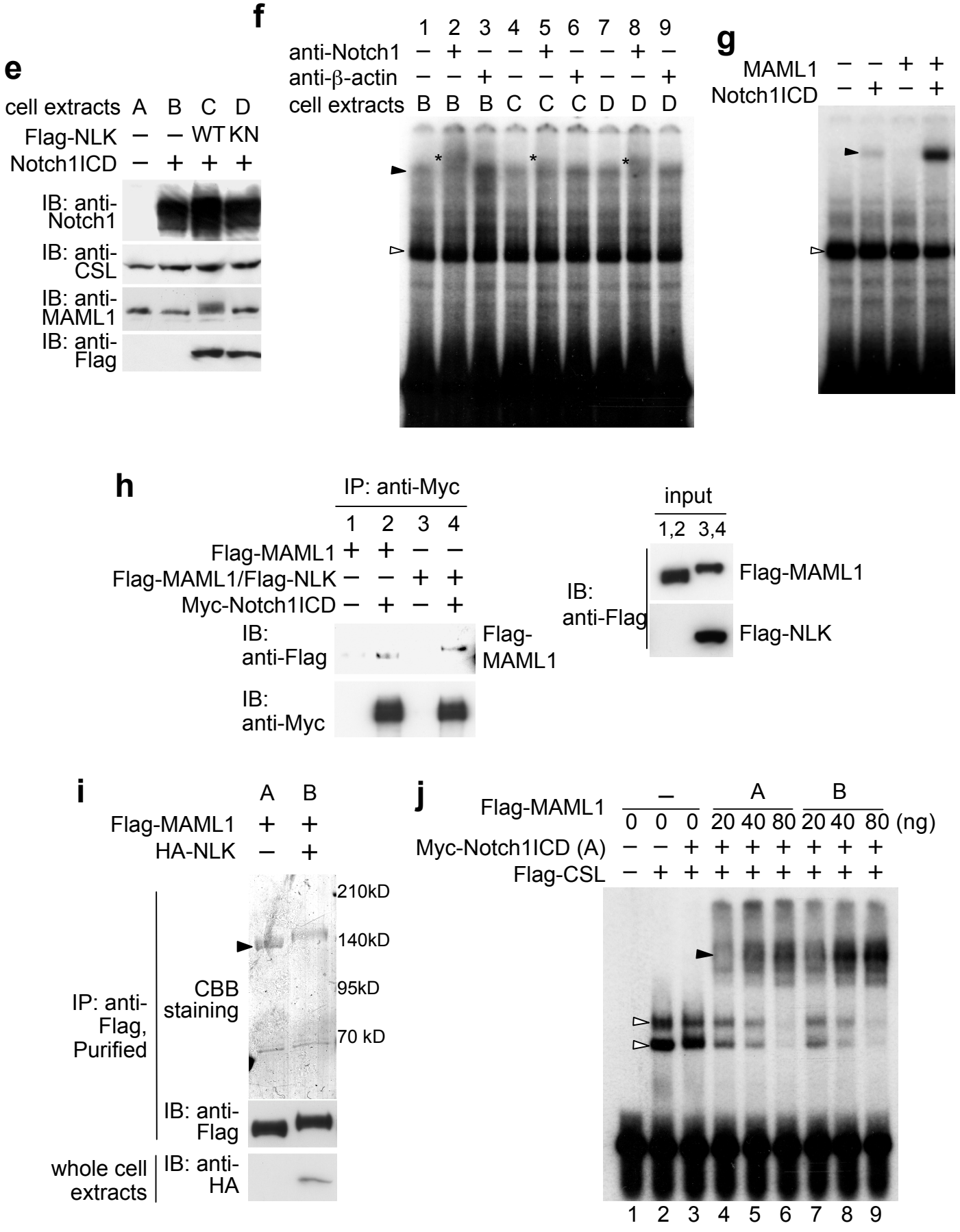

Figure S9 Ishitani & Itoh

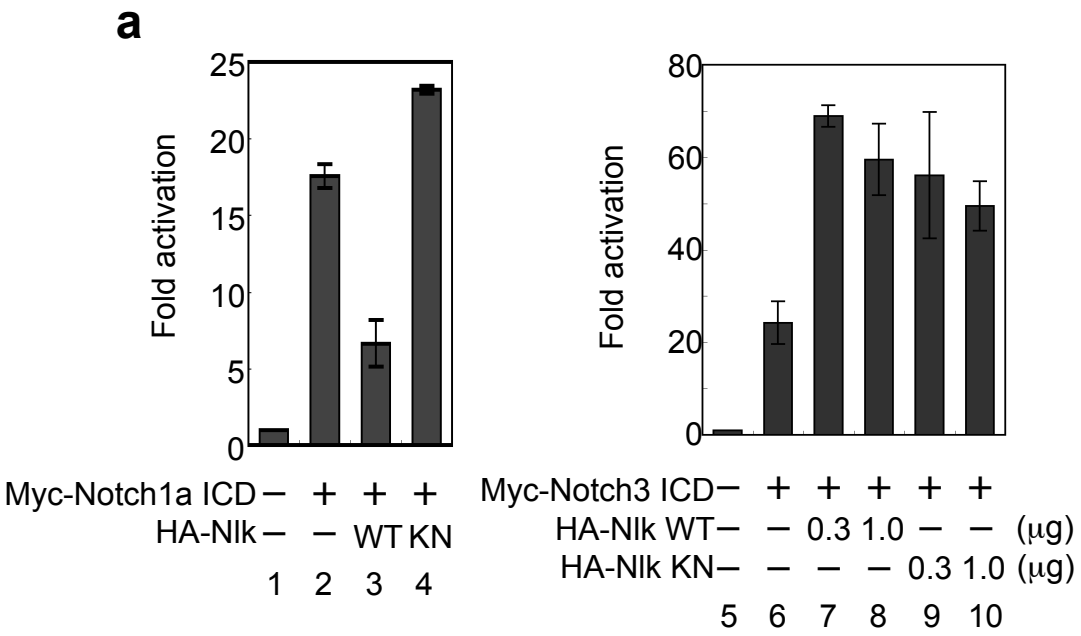

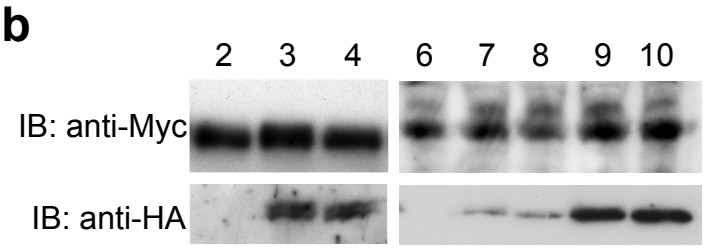

Figure S10 Ishitani & Itoh

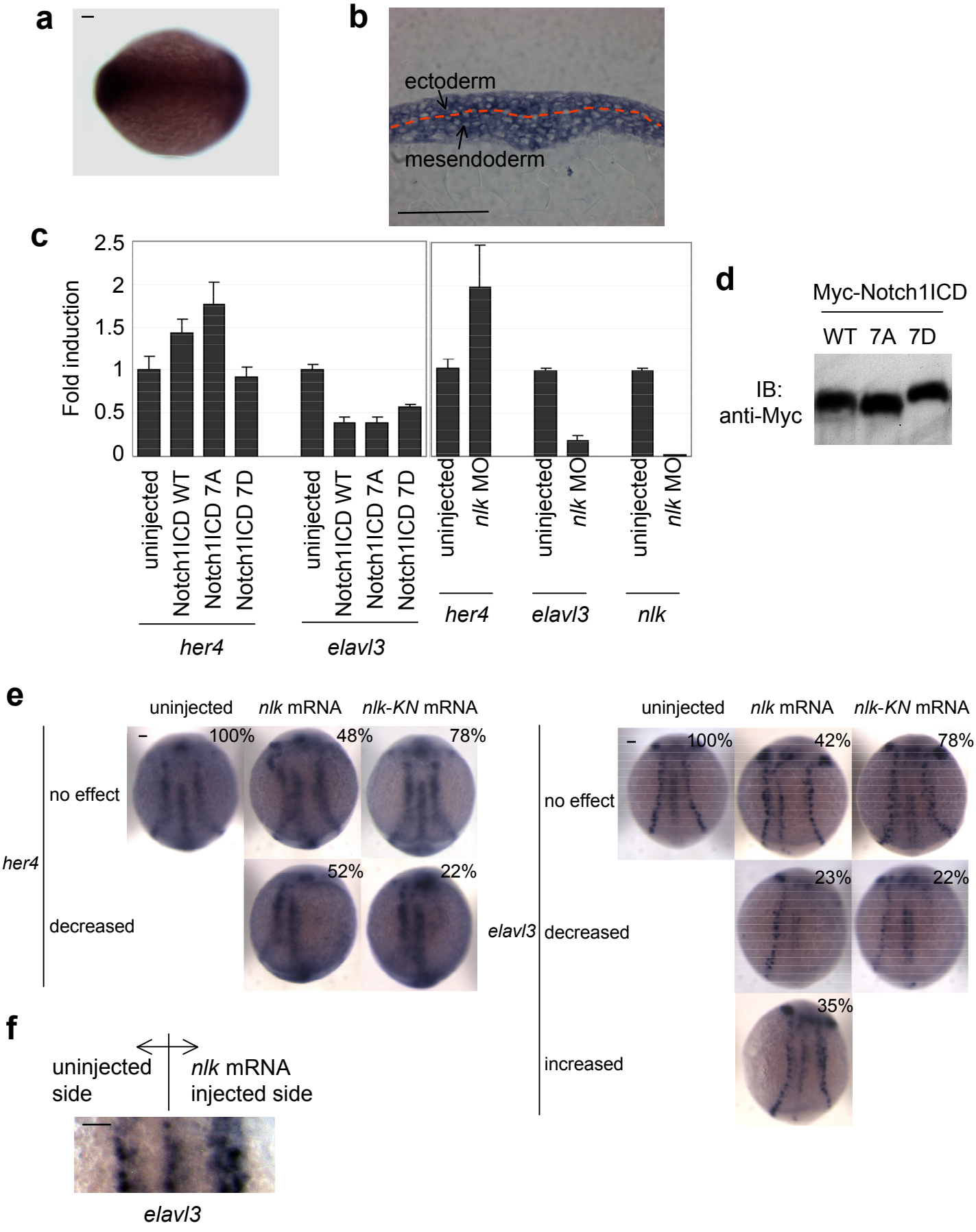

Figure S11 Ishitani & Itoh

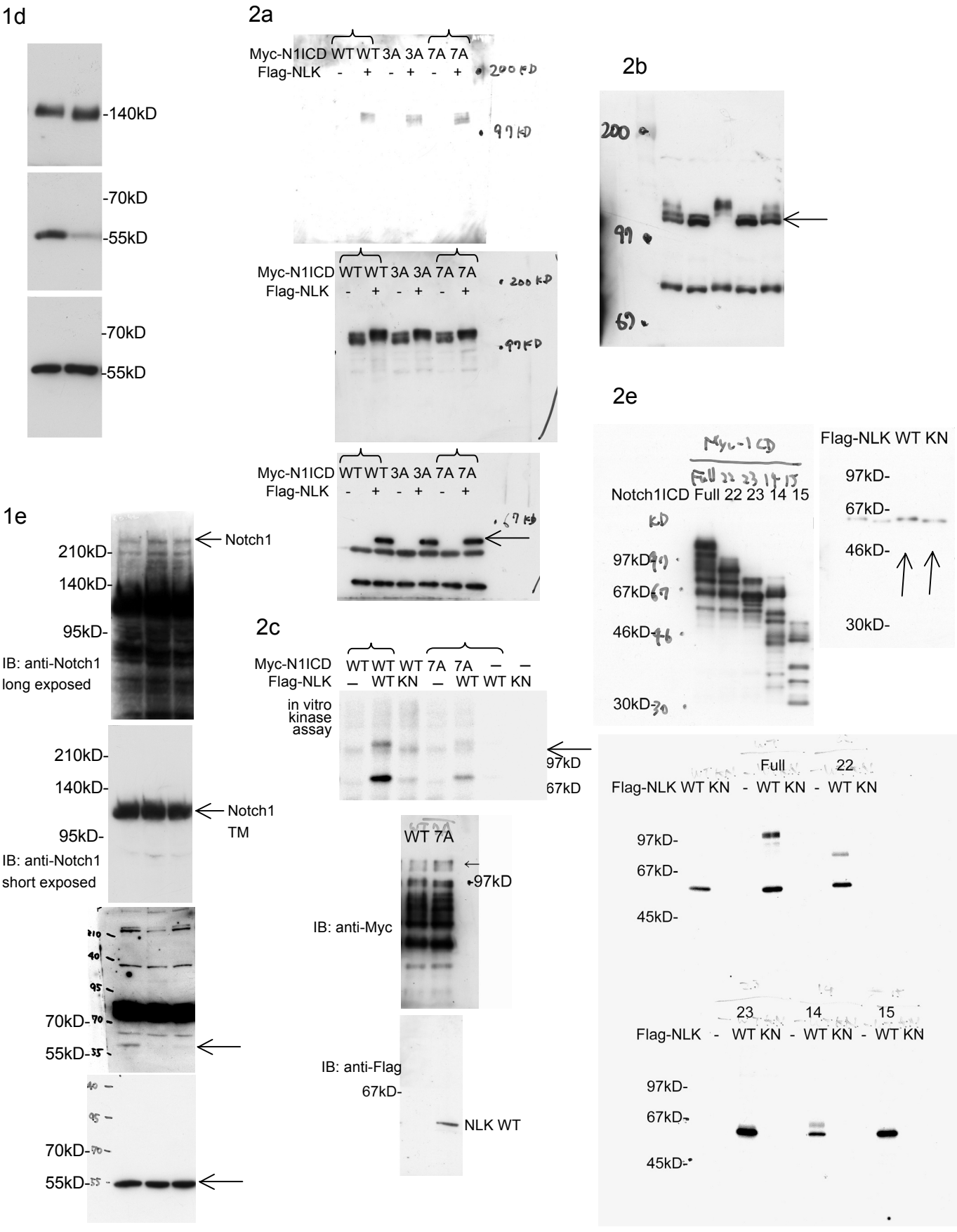

Figure S11 (continued) Ishitani & Itoh

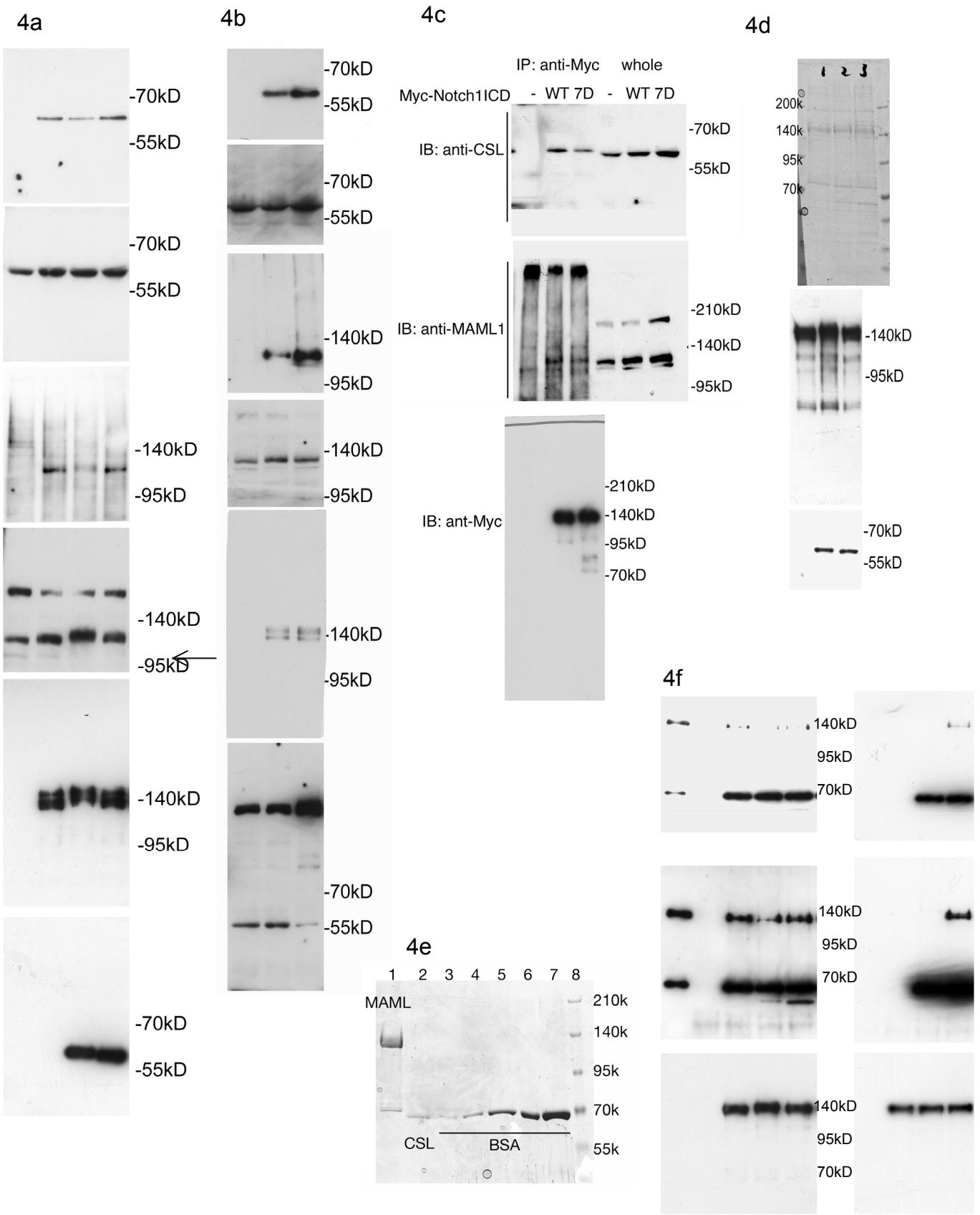

Table S1 Ishitani & Itoh

Effects of MOs on the expression of *her4*, *hes5*, and *elavl3*.

	uninjected	*nlk* MO	*notch1a/3* MOs	*nlk* MO + *notch1a/3* MOs
normal *her4* expression	100% (n=114)	35% (n=49)	18% (n=45)	23% (n=61)
increased *her4* expression	0% (n=114)	65% (n=49)	0% (n=45)	0% (n=61)
decreased *her4* expression	0% (n=114)	0% (n=49)	82% (n=45)	77% (n=61)
normal *hes5* expression	100% (n=63)	28% (n=54)	26% (n=54)	30% (n=54)
increased *hes5* expression	0% (n=63)	72% (n=54)	0% (n=54)	0% (n=54)
decreased *hes5* expression	0% (n=63)	0% (n=54)	74% (n=54)	70% (n=54)
normal *elavl3* expression	100% (n=114)	34% (n=61)	2% (n=43)	6% (n=77)
increased *elavl3* expression	0% (n=114)	0% (n=61)	98% (n=43)	94% (n=77)
decreased *elavl3* expression	0% (n=114)	66% (n=61)	0% (n=43)	0% (n=77)